Graduation thesis

Characterisation of the LEDs and InGaAs detector of the handheld plastic scanner

Internship coach: R. Buning
Company supervisor: J. De Vos
Physics supervisor: H. Van Hoorn

Queena L.D. Rijke (18098258)
May 23, 2023

Abstract

Contents

List of Figures

Abbreviations

CB Conduction band. 9, 11

EHP Electron-hole pair. 12–14

FWHM Full Width Half Maximum. 17, 28–31

HDPE High-Density PolyEthylene. 1, 3, 6, 21–23, 25, 33

InGaAs Indium Gallium Arsenide. 2, 3, 13, 14, 16, 17, 20, 21, 27–29, 31

IR Infrared. 1, 2, 4, 5, 7, 12

LDPE Low-Density PolyEthylene. 21–23, 25, 34

LED Light Emitting Diode. 2, 3, 8–12, 16–19, 21, 23–25, 28–33, 35

NIR Near-Infrared. 4, 5, 16–25, 28, 31–33

PET PolyEthylene Terephthalate. 1, 3, 21–23, 25

PP PolyPropylene. 1, 3, 21–23, 25

PS PolyStyrene. 1, 3, 21–23, 25

PTFE Polytetrafluorethylene. 7, 8, 21, 23, 25

PVC Poly Vinyl Chloride. 1, 3, 6, 21–23, 25, 33

QE Quantum Efficiency. 14

SCL Space Charge Layer. 13

SNV Standard Normal Variation. 21, 32

VB Valance band. 9, 11

1 Introduction

Plastic pollution is one of the most pressing problems worldwide. The gathering of plastics in nature is negatively affecting all living surroundings, humans and animals alike. The popularity of plastics accelerated after World War II, because of its versatility, durability and affordability. Plastic has made space travel possible, revolutionised medicine and improved our safety with helmets and car lights. However, plastics are also used for everyday consumption, such as straws, grocery bags, bottles and more. Since the production and consumption of plastics are faster than the degradation, the plastics are accumulating and ending up on land or in various waters. The manufacturing of plastic increases exponentially from 2.3 million tons in 1950 to 448 million tons in 2015, and is expected to be doubled by 2050. The pollution is mostly visible in the developing countries, where recycling systems are inefficient or nonexistent. [1–3]

The collecting and sorting process prior to recycling have proved especially problematic, manly in the developing countries. When sorting plastic, the plastic recycling codes can be checked located on the plastic material as triangles made of arrows. Within these arrows a number is given which states the type of plastic.

Figure 1.1: The plastic resin codes. [4]

Each type of plastic is recycled with a different method, as each type consists of a different molecular structure. The five most common types of plastic are PET (PolyEthylene Terephthalate), HDPE (High-Density PolyEthylene), PVC (Poly Vinyl Chloride), PP (PolyPropylene) and PS (PolyStyrene). To distinguish the different types of plastic with a higher quality, infrared (IR) spectroscopy can be used. Sorting the plastic by means of IR spectroscopy is, however, an expensive way to sort the different types of plastic, but this method can identify over 75% commonly used types of plastic. The different types of plastic can be identified by IR absorbance or IR reflectance. [2,5]

Being able to separate the different types of plastic in a high-quality manner is important to ensure a successful recycling process. Jerry de Vos discovered during his thesis research that this process is the most time consuming and labour-intensive. Therefore Jerry made it his mission to develop a spectroscopy based technology that

can separate the five most common types of plastic, for those in developing countries. The technology that is applied to develop the handheld plastic scanner is based on the technology developed by Armin Straller [6]. To increase the development process, the project has been set up as an open source project. All documentation, designs and progress is available at plasticscanner.com. [2, 7]

In spectroscopy, a broadband light source is used to illuminate the sample, after which the absorption or reflection spectrum is detected on a detector. Where the detector receives the intensity by wavelength. The handheld plastic scanner uses a select number of LEDs in the IR spectrum, each with a different wavelength, as the illumination light source and an InGaAs detector as the detector. The wavelength selection is thus done at the light source as opposed to between the light source and the detector. Since the wavelength selection is made prior to the illumination, it is necessary to investigate whether the correct wavelengths have been selected to identify the different types of plastic. Next to using a less expensive light source for the plastic scanner development, a less expensive detector is used in the development. This involves researching whether the InGaAs detector can detect the wavelengths emitted by the LEDs. Besides the characterisation of the spectroscopy components, the influence of colour in plastic will be researched by means of the reflection spectra. [8, 9]

In order to determine whether the correct LEDs and detector are used and whether added colour affects the reflectance spectra of plastic, this report first describes the properties of plastic, LEDs and InGaAs detector and the operation of spectroscopy in the Theory. The method for the experiments is discussed in the Method after which the results are discussed. A conclusion is drawn from the results. Additional information can be found in the Appendices.

2   Theory

This chapter discusses the theory of the molecular structure of plastic, spectroscopy and the characteristics of LEDs and the InGaAs detector.

2.1   Molecular structure of plastic

Plastics are made out of polymers and can either occur as a natural or synthetic product. A polymer consists of multiple monomers bonded together. The plastics can be shaped when soft and can hold the shape when hardened [10–12]. Five of the most common plastics are: PET (PolyEthylene Terephthalate), PVC (Poly Vinyl Chloride), PP (PolyPropylene), PS (PolyStyrene) and HDPE (High-Density PolyEthylene) and are presented in figure 2.1.
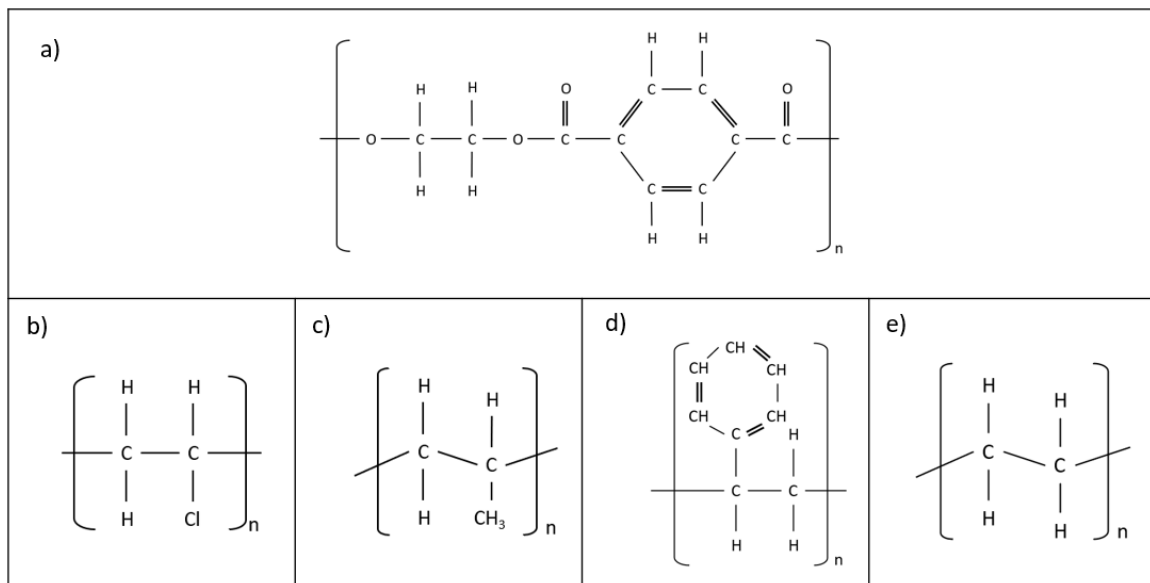
Figure 2.1: The different molecular structures of the five most common types of plastic. a) shows the structure of PET, b) shows the structure of PVC, c) shows the structure of PP, d) shows the structure of PS and e) shows the structure of HDPE. [13–17]

The molecular structures experience internal vibrations. Depending on the bonding between the atoms of the molecule, the molecule can vibrate in different directions. There are two different types of vibrations, bending and stretching. The bending vibrations occur in four different directions, presented in cell A in figure 2.2. The stretching occur in two different directions, also presented in figure 2.2 in cell B.

3
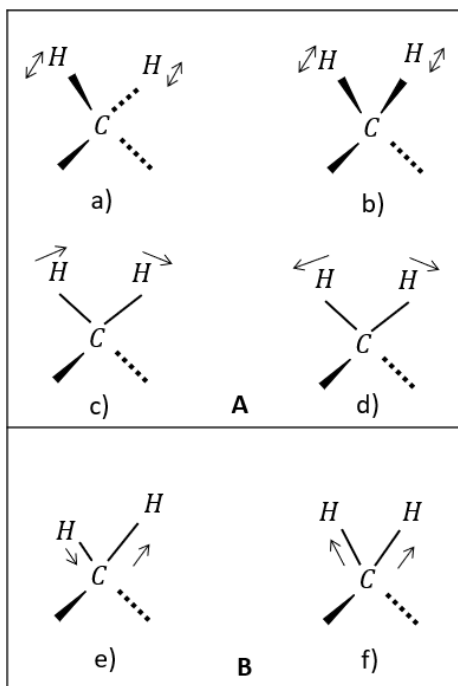
Figure 2.2: The bending vibrations are a) twisting, b) wagging, c) rocking and d) scissoring, presented in cell **A**. e) and f) are the asymmetrical and symmetrical stretching, presented in cell **B**.

These vibrations are known as normal modes, independent molecule vibrations. The frequencies of the normal modes are determined by the mass of the molecule atoms and its force constants. Multiple normal modes with the same frequency can occur in a molecule because of the symmetry inside the molecule. A molecule can absorb IR radiation when the normal mode vibrations cause a change in dipole moment. The vibration is then active-infrared. [18]

Each absorbance creates absorption bands forming an absorption spectrum. The C-H, O-H, N-H and C-O bonds characterise specific types of plastic by the absorbance in the NIR spectrum. The absorbance bands in figure 2.3 are of the fundamental normal modes. When the monomers are bound into polymers, the vibrations become weaker and the absorbance bands shift to the near infrared (NIR).
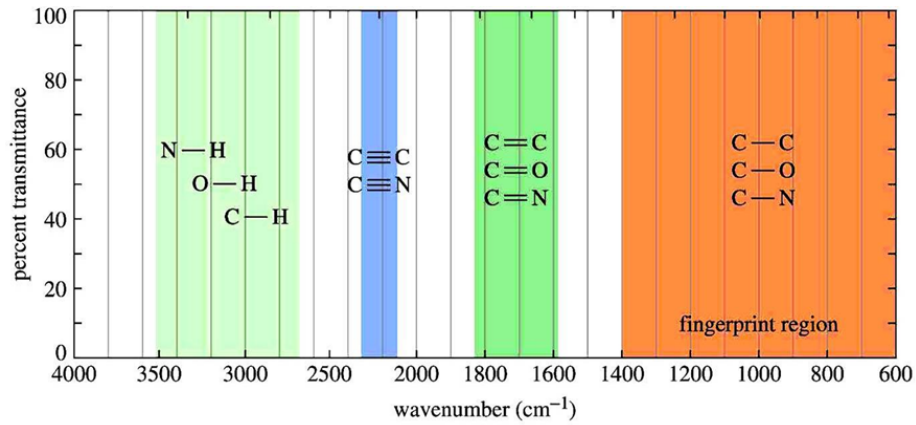
Figure 2.3: The absorbance bands of specific C-bonds at a wavenumber range in the IR spectrum. [19]

The IR spectrum ranges from 750 nm to 50 µm, in which the Near-infrared (NIR) ranges from 750 nm to 2.5 µm. These wavelengths are quite high and are therefore often written in wavenumbers. The wavenumber is a characterisation of the radiation in waves per centimetre, denoted by σ. The wavenumber,

$$\sigma = \frac{1}{\lambda} \tag{2.1}$$

in which λ is the wavelength in cm. The convenience of a scale in wavenumber is the linearity in energy. [18]

Each type of plastic has multiple C-bonds which form a absorption spectrum. Figure 2.4 shows the absorption spectra of the different types of plastic. The spectra are shown with an offset to give a clear distinction between the types of plastic.
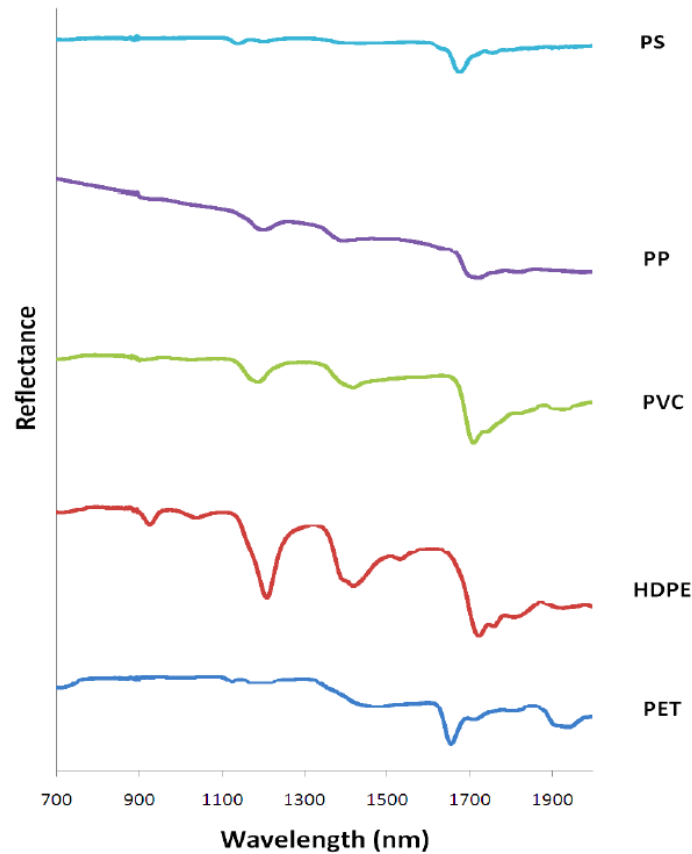
Figure 2.4: The reflectance of five of the most common types of plastic. The spectra are plotted with an offset to avoid interference and enhance clarity. The signature dips of the types of plastic are most present between 1100 nm to 1500 nm and around 1700 nm wavelength. [20]

Figure 2.4 shows that all the plastic types experience absorption between 1100 nm to 1500 nm and around 1700 nm. HDPE can be distinguished from PVC because of the absorption dip seen around 950 nm. The different spectra produced by the molecules of the plastics can be used for identification through reflectance spectroscopy. [20]

ATOMEN EN SMELTPUNT.

2.2   Infrared spectroscopy

Spectroscopy is the study of the interaction between electromagnetic radiation and matter. The matter can absorb, reflect and transmit electromagnetic radiation depending on the frequency of the normal modes. The measuring of the electromagnetic radiation absorbed or emitted when atoms, molecules or ions of the matter undergo a state change, is called spectrometry. The measuring is done with a spectrometer, which consists of three basic elements. A light source, an element to isolate a narrow range of wavelengths and a detector. A spectrometer detects the transmission or

reflection of a sample. The absorbance of a substance is measured by transmission and can be determined using the Beer-Lambert law,

$$A = \log_{10} \frac{I_0}{I_t} = -\log_{10} T = \varepsilon bc \tag{2.2}$$

in which I_0 is the incoming intensity in W m^{-2}, I_t is the transmitted intensity in W m^{-2}, T is the transmission, ε is the molar absorption coefficient in l mol^{-1} cm^{-1}, b is the path length in cm and c is the concentration in mol l^{-1}. [18, 21, 22]

The concentration or path length of a substance affects the amount of transmission. A measurement with a transmission between 30% and 70% falls within the accuracy range. A transmission higher than 75% indicates that the concentration is low or the path length is small.

Infrared (IR) spectromerty uses transmission or reflection to give an absorbance spectrum, by illuminating the sample with a light source in the IR spectrum. The difference in the setup determines if the reflection or transmission is measured by the detector in the spectrometer. An illustration is given in figure 2.5
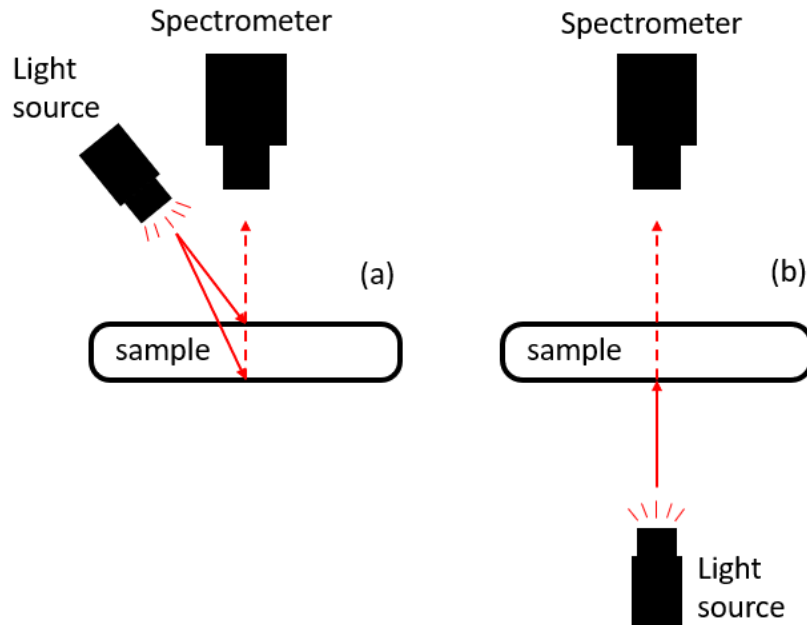

Figure 2.5: The setup of the spectrometer to detect reflection or transmission. (a) shows the setup of to detect reflection and (b) shows the setup of to detect transmission.

The reflectance of a sample is determined by dividing the reference reflection of a reference tile, mainly made of PTFE, with the reflection of the sample.

$$R = \frac{I_r}{I_0} \tag{2.3}$$

in which R is the reflectance, I_r is the intensity measured from the sample in counts and I_0 is the reference intensity of the reference tile in counts. PTFE is used because of the material's diffusivity. As a result, most of the illumination light is expected to be reflected.

When measuring the spectra of the different types of plastic, it is expected that the characteristics of the spectra will correspond with the characteristics shown in figure 2.4. It is also expected that the progression of the spectra will stay the same when measuring different colours of the same type of plastic, apart from dark colours where the progression will diminish. [8, 18, 20]

2.3   Light-emitting diodes

Light-emitting diodes (LEDs) are pn-junction diodes in which photon emission is generated as a result of a electron-hole pair recombination. A pn-junction diode is formed when a n-type semiconductor is joined to a p-type semiconductor. An n-type semiconductor is a doped crystal in which the negatively charged electrons carry the electric current, as a result of an excess in electrons. A p-type semiconductor is a doped crystal in which the electric current seems to be carried by the positively charged holes that the electrons leave when moving to a previous hole, as a result of a shortage in electrons. [23]

Both semiconductors do not have a net charge. As a pn-junction a few of the electrons of the n-type fill the holes of the p-type, which causes the n-type to become positively charged and the p-type to be negatively charged. This region of depleted free carriers is called the depletion region and causes a potential difference inside the pn-junction, a built-in voltage (V_0). The depletion region decreases when a forward bias is applied. Figure 2.6 demonstrates the flow of electrons and holes in equilibrium (a) and applied to a forward bias (b).
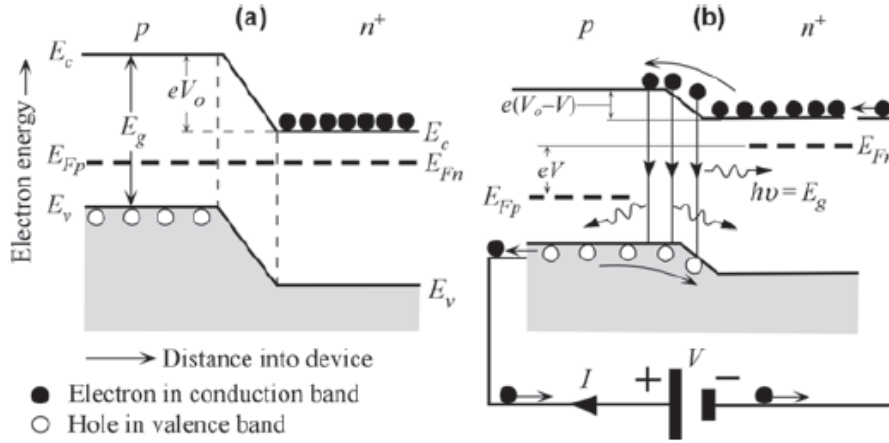
Figure 2.6: A schematic drawing of a pn-junction. The black circles represent the electrons in the conduction band and the white circles represent the holes in the valence band. (a) shows the pn-junction in equilibrium and (b) shows the pn-junction with an applied forward bias, in which the negative side of the power supply is connected to the n-type and the positive side of the power supply is connected to the p-type. [23]

The free electrons are located in the conduction band (CB). The region in which the black circles (electrons) are located in figure 2.6. When the depletion region (dotted lines) between the conduction band and the valence band (VB) becomes smaller, the electrons can fill a hole in the valence band. The region in which the white circles (holes) are located in figure 2.6. The 'falling' of the electron from the bottom of the CB to the top of the VB is called recombination. During the process of recombination energy is released as a photon. A spontaneous emission of a photon. When connected to a forward bias a flow of spontaneous photon emissions takes place. The depletion region is then called the active region. The photons emitted in the active region have to escape the LED structure without being reabsorbed by the semiconductor material. Therefore the p-type side of the pn-junction needs to be very narrow, or a heterostructure can be used.

To create a heterostructure multiple heterojunctions are combined. A heterojunction are two different semiconductor crystals, with different bandgap energy, joined together. In this case a pn-junction. By combining pn-junctions a dielectric waveguide can be formed to guide the emitted photons out of the active region. The difference between the bandgaps can be increased by altering the refractive index of the semiconductor material and in doing so the LED intensity increases. Figure 2.7 shows an example of a double heterostructure.
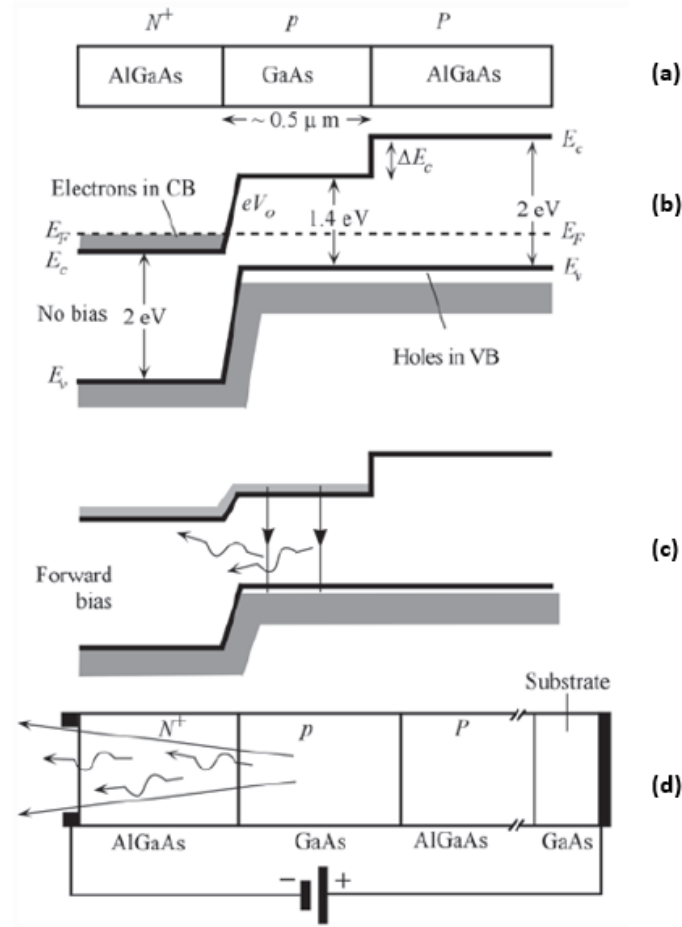
Figure 2.7: A simplified double heterostructure diode. (b) shows an energy band diagram in which the features are exaggerated, (c) shows a forward-biased energy band diagram, (d) a forward-biased LED, in which the escaping of the emitted photons is illustrated. [23]

Not all light rays can leave the heterostrucure waveguide, because of total internal reflection on the semiconductor-air interface. By reshaping the surface of the semiconductor more light can leave the structure. A dome or hemisphere could be used to change the angle in which the light strikes the semiconductor-air interface and therefore more light can be emitted. More common used techniques to increase emission of light is to encapsulate the semiconductor within a transparent plastic medium or to texturise the surface. A distributed Bragg reflector could also be used to increase the extraction ratio of the LED's wavelength or a resonant cavity could be used as a LED design. These LED designs are shown in an exaggerated form in figure 2.8.
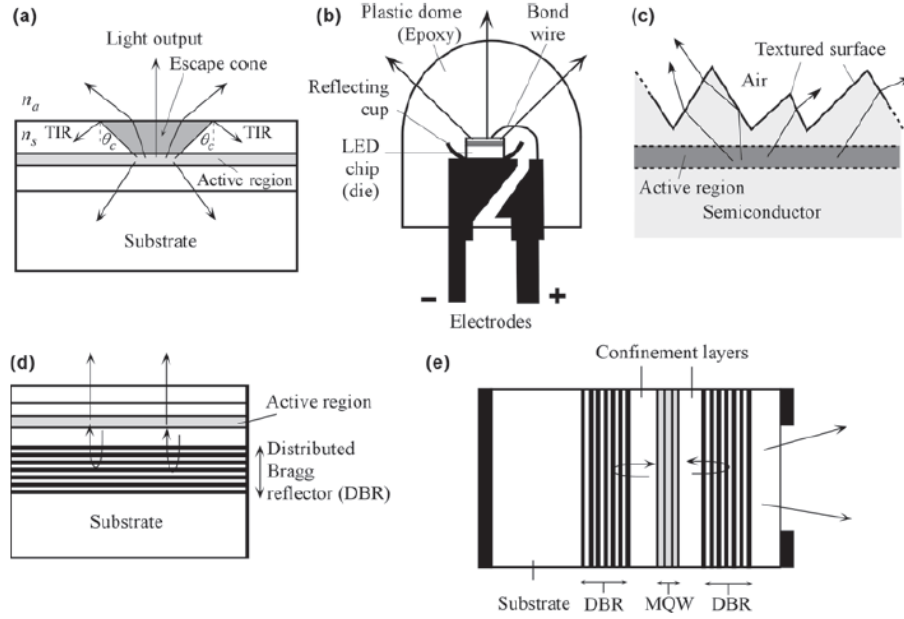
Figure 2.8: Five different designs to increase the intensity of a LED. The plastic dome (b) is used to increase the intensity of the LEDs used in the plastic scanner. [23]

The plastic dome design (2.8b) is used for the design of the LEDs used in the plastic scanner.

The output spectrum of the LED is next to the dependence of the semiconductor material and the structure of the pn-junction also dependent on the dopant concentrations. The semiconductors are typically not heavily doped to generate photons with a higher energy than E_g and to acquire a sharp edge between the energy of the CB and the energy of the VB. The emission of the output spectrum can be described as follows,

$$h\nu_0 \approx E_g + \frac{1}{2}k_B T$$
$$h\Delta\nu = mk_B T$$

(2.4)

in which

h	constant of Planck	$6.626 \cdot 10^{-34}$ Js
ν_0	peak emission frequency	Hz
E_g	bandgap energy	eV
k_B	Boltzmann constant	$1.3807 \cdot 10^{-23}$ JK^{-1}
T	temperature	K
$\Delta\nu$	spectral width	Hz
m	numerical factor	-

11

The value for m for many LEDs is $m \approx 3$. Typically the value varies between 1.5 and 3.5. Equation 2.4 can be written in terms of wavelength λ_0 or spectral width $\Delta\lambda$. Both wavelength and spectral width increase with an increase in temperature. This can be seen in figure 2.9. [23, 24]
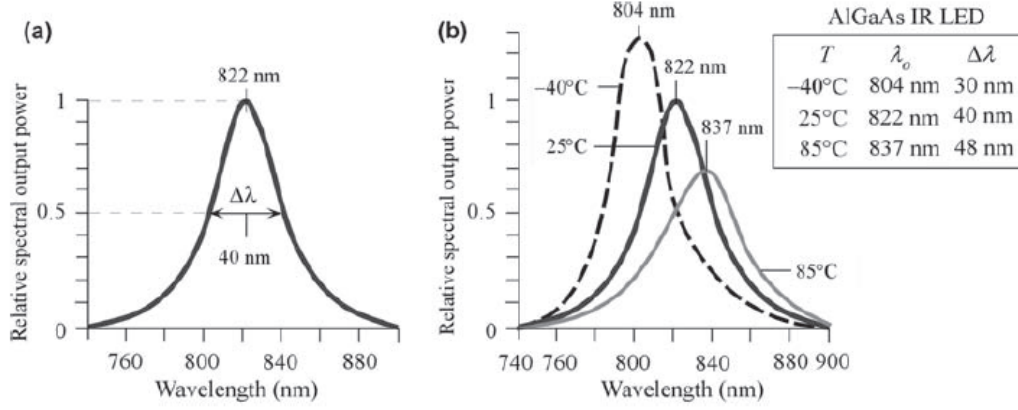
Figure 2.9: The output spectrum of an IR AlGaAs LED. (a) shows the typical out put spectrum of the AlGaAs LED and (b) shows the shifting of the output spectrum with increase in temperature. [23]

2.4   InGaAs detector

A photodiode is a pn-junction in which photons are absorbed to generate electron-hole pairs (EHP). Compared to the LED pn-junction the photodiode has a p^+-type as to the n^+-type of the pn-junction of the LED. The plus-sign in the p^+-type, means that the concentration of acceptors is greater than the donor concentration in the n-type. The pn-junction of the photodiode too has a built-in voltage. By applying a reverse bias to the pn-junction the depletion region becomes greater, which gives more space for EHP photogeneration.

A free EHP is created when a photon is absorbed in the depletion region. The electron and hole drift toward the opposite side of the pn-junction and generate a current, the photocurrent I_{ph}. The duration of the current is as long as the electron and hole drift. The electron and hole drift are visually represented in figure 2.10 after the absorbance of a photon under a reverse bias.

Figure 2.10: A reverse biased pn-junction in which a free EHP is generated by the absorbance of a photon. The photogeneration takes place in the depletion region (SCL). The free electron and hole drift causing a photocurrent I_{ph}. [25]

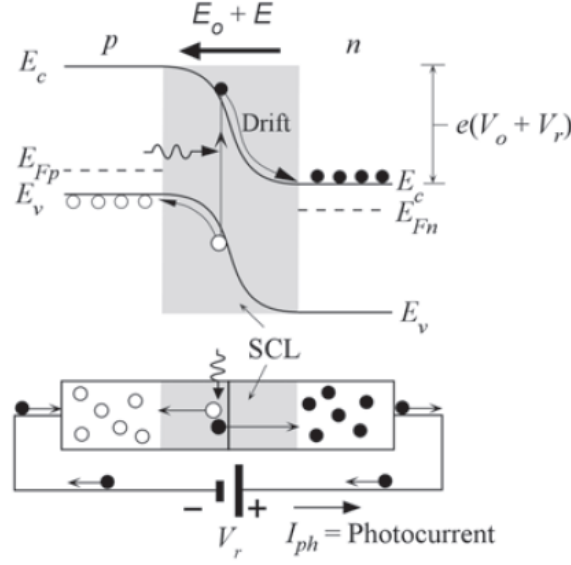For the photon to be absorbed and generate an EHP, the energy of the photon needs to be at least equal to the energy of the bandgap E_g of the semiconductor material. The wavelength of the photon therefore depends on the bandgap energy. The threshold wavelength of the photon can be determined using the following equation:

$$\lambda_g(\text{µm}) = \frac{1.24}{E_g(\text{eV})} \tag{2.5}$$

in which λ_g is the threshold wavelength in μm and E_g the bandgap energy in eV. The plastic scanner uses an InGaAs photodiode. The values of the threshold wavelength and the bandgap energy corresponding to the InGaAs detector are $E_g = 0.75$ eV and $\lambda_g = 1.65$ µm.

The light intensity of the photons with a wavelength shorter than λ_g decays exponentially over a distance into the semiconductor. The distance over which the most absorption takes place is called the penetration or absorption depth (δ). The absorption depth can be determined through the absorption coefficient.

$$\delta = \frac{1}{\alpha} \tag{2.6}$$

in which α is the absorption coefficient in m^{-1}.

With a large absorption coefficient the photogeneration will take place near the surface of the p^+-layer and when the absorption coefficient is too small the number of generated EHPs decreases in the depletion region. A greater efficiency is reached

when the photogeneration takes place in the depletion region. The efficiency of the absorption in the depletion region can be determined with the following equation,

$$\eta_e = \frac{I_{ph}/e}{P_0/h\nu} \qquad (2.7)$$

in which η_e is the device quantum efficiency (QE), I_{ph} is the photocurrent in A and P_0 is the incident optical power in W.

Not all incident photons generate free EHPs that are collected to induce a photocurrent, when absorbed on the photodiode. Some disappear by recombination, get trapped or reflect on the air-semiconductor interface. The performance of the photodiode is characterised by its responsivity, photocurrent per incident optical power.

$$R = \frac{I_{ph}}{P_0} = \eta_e \frac{e\lambda}{hc} \qquad (2.8)$$

in which R is the responsivity in A/W. As seen in equation 2.8, the responsivity is depended on the wavelength. It is therefore often represented in a R vs. λ graph, which is usually provided by the manufacturer. The theoretical responsivity of the InGaAs detector is presented in figure 2.11.
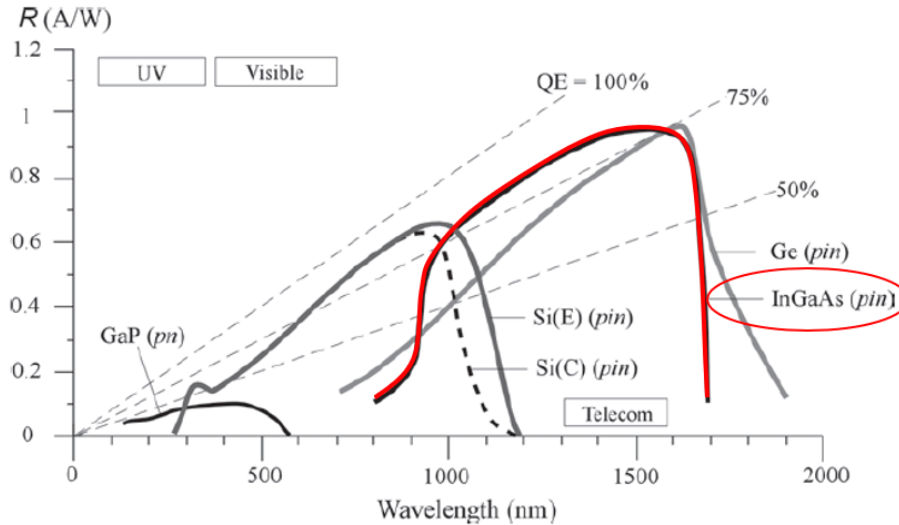
Figure 2.11: The red line is the responsivity of the InGaAs detector. The detection range is from 800 nm to 1700 nm. [25]

The shape of the curve in figure 2.11 is depended on the structure of the device, the absorption coefficient and the QE.

The responsivity of the InGaAs detector in figure 2.11 is of a pin photodiode. The biggest advantage of a pin photodiode is the wider depletion region allowing a larger

amount of photogeneration can take place. For this reason the responsivity is better than a pn-junction photodiode. [25]

3 Method

The plastic scanner is a spectrometer which illuminates the sample with 8 different LEDs. Each LED has a different wavelength inside the NIR spectrum. The plastic sample is illuminated in turns by each LED. The internal design of the plastic scanner is presented in figure 3.1.
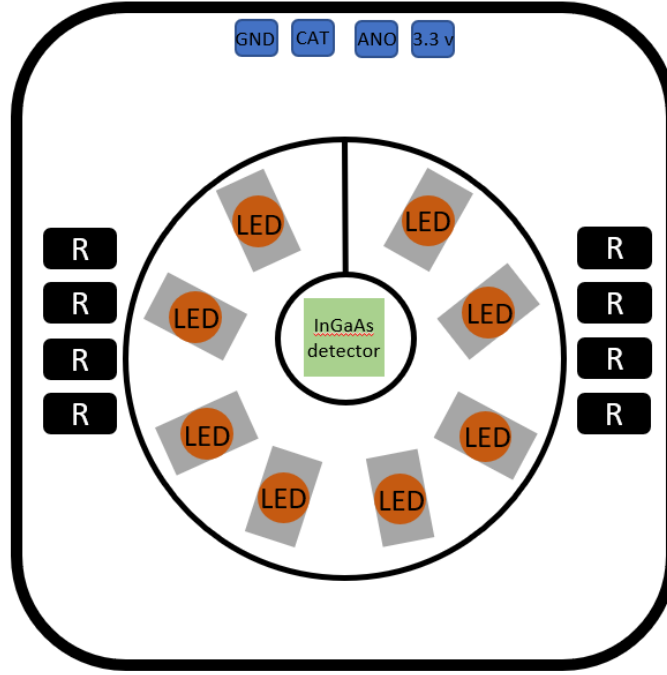
Figure 3.1: The internal design of the spectroscopic side of the plastic scanner. The InGaAs detector is surrounded by 8 LEDs, each emitting light in an different wavelength. The resistors for the LEDs are placed on the sides of the board (R). The Arduino, to manage the LEDs and analyse the reflected spectra collected from the InGaAs detector, is connected via the four connectors at the top of the board. The GND and 3.3v deliver the voltage to the board and the CAT and ANO are the connectors for the detector. The outer circle around the LEDs is the spacer between the plastic samples and the LEDs, usually 10 mm high. The inner circle around the InGaAs detector is used to block any direct light from the LEDs into the detector, usually 4 mm high.

A side view of the internal design to show the placement of the spacer is presented in figure 3.2.

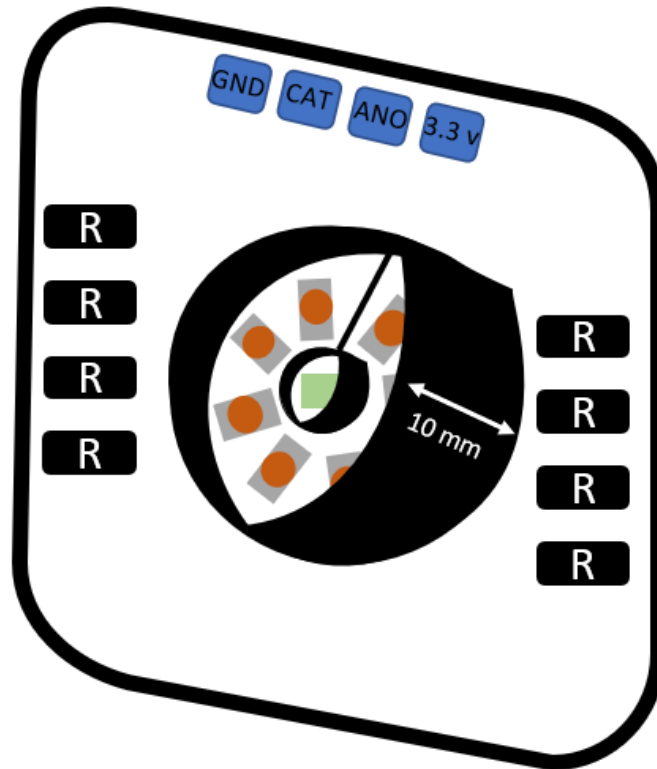Figure 3.2: A side view of the internal design of the spectroscopic side of the plastic scanner. The LEDs are surrounded by a 10 mm high spacer. The InGaAs detector is surrounded by a 4 mm high spacer to block any direct light emitted from the LEDs.

A discrete spectrum of a plastic sample is measured at specific wavelengths. To determine if the plastic samples can be identified using the plastic scanner, a reference of the spectra of the plastic samples is made using a NIR spectrometer and a broadband light source for illumination. By characterising the components, the LEDs and the InGaAs detector, the efficiency and accuracy of the plastic scanner can be determined.

First the characterisation of the LEDs and InGaAs detector will be discussed. Second the measuring method to determine the spectra of the plastic samples will be discussed.

3.1   LED characterisation

Of most LEDs the spectra, FWHM and peak wavelengths are known from the data sheet. Because not all data is known from all LEDs, the spectra will be measured using a spectrometer as detector. The equipment needed to build the setup are as follows:

- Optical multimode fibre (FC-UVIR400-1-ME)
- NIR LED development board

- LED development board ($\lambda = 500$ nm?)

- Cable to connect the development board to the power supply

- Computer to manage the LEDs and to run the Avasoft8 software

- Optical plate

- Avantes NIR spectrometer (AVASPEC-NIR256-2.0TEC)

- Avantes spectrometer (AVASPEC-ULS2048CL-EVO-RS)

- Lens (Thorlabs LSB04-A $\varnothing$1" N-BK7, $f = 25.4$ mm)

- USB-A to USB-B cable

- SMA mounts to hold the fibre ends

- Lens mount

Setup

The setup to characterise the LEDs is built according to figure 3.3. The lens is placed between the LED development board and the first fibre mount. An optical multimode fibre can be attached to the second fibre mount or the NIR spectrometer. The dotted line suggests the different connections of the fibre. It can either be connected to the second fibre mount or the spectrometer.
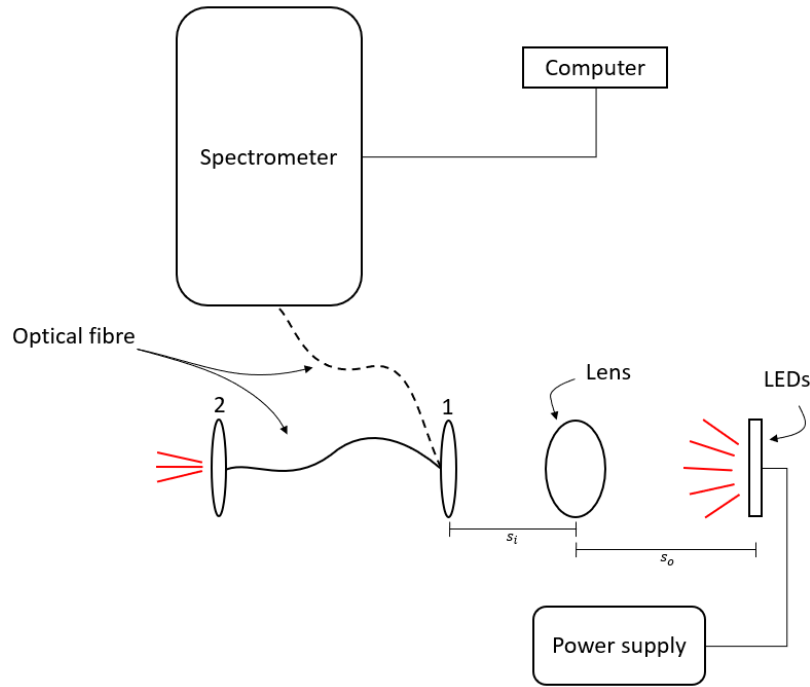
Figure 3.3: A schematic top view of the setup to determine the spectra of the LEDs. The lens is placed at an object distance s_o and the fibre is placed after the lens, connected to fibre mount 1, at an image distance of s_i. The fibre can be connected to the NIR spectrometer or fibre mount 2. The NIR spectrometer is connected to a computer containing AvaSoft8 software.

To measure the spectra of the LEDs, the light of the LEDs is focused by a lens into the fibre which is connected to the spectrometer. By using a LED development board with LEDs in the visible spectrum, the LEDs can be aligned. The LED development board is connected to a board with switches. Each switch lights a different LED on the board. The power supply is set at a voltage of 3.3 V. When a LED is correctly aligned the light is transmitted to through the fibre and is visible on a screen or a finger held before fibre mount 2. After alignment the LEDs within the visible spectrum are replaced with the LEDs in the NIR spectrum. The fibre is then connected to the spectrometer and the spectrum of the aligned LED can be measured. The integration time and the average in the AvaSoft8 programme for the NIR spectrometer will be determined by aligning the 1550 nm LED into the spectrometer and press the auto configuration button . The wavelength range goes from 1000 nm to 2000 nm. The integration time and the average in the AvaSoft8 programme for the spectrometer will be determined by aligning the 940 nm LED into the spectrometer and press the auto configuration button . The wavelength range goes from 300 nm to 1100 nm.

The data is manually saved in Excel-documents and plotted using python.

19

3.2 InGaAs detector characterisation

The characterisation of the InGaAs detector cannot be improved compared to the responsivity given in the data sheet. Hence the data from the data sheet will be used for the charaterisation of the plastic scanner.

Setup

The plotted data of the responsivity of the detector has been extracted using an online program named WebPlotDigitizer [26]. Figure 3.4 shows a picture of the program.
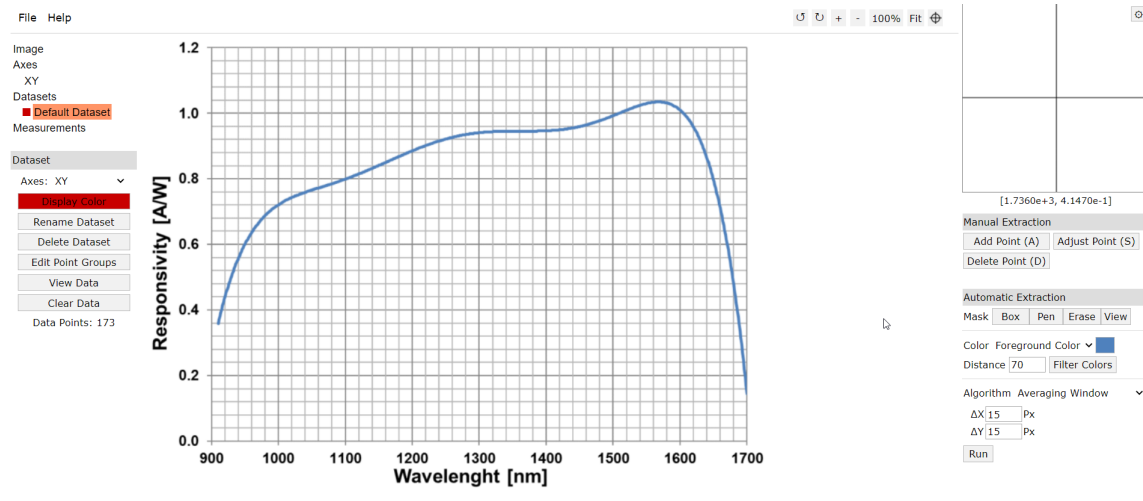

Figure 3.4: A screenshot of the WebPlotDigitizer program. It shows the uploaded graph in the middle. The way to extract the data from the uploaded graph are presented on the right side. On the left side, the extracted data can be viewed and downloaded.

Within the program an image of the graph given in the data sheet is uploaded. To determine the values of the curve of the graph, the minimum and maximum values of the x- and y-axis are determined by selecting and entering the minimum and maximum values into the designated areas on the website. Once the outline of the graph is established the curve of the responisivity is selected using the pen function. The colours are then filtered on an distance value of 70, using the colour picking function to determine the colour code of the curve. The ΔX and ΔY are set on 15 Px. Then the program can be run and the data is given in dots on the graph and can be viewed by clicking on the "View Data" button. The acquired data can be adjusted in the formatting and saved as a CSV-document.

3.3 NIR reflection spectroscopy

The spectra of the plastic samples are measured in three different ways. As a reference the spectra are measured using a halogen lamp as the illumination source and a NIR

spectrometer as the detector. The spectra are also measured using the LEDs as the illumination light source with the NIR spectrometer as the detector. In final the spectra are measured with the plastic scanner using the LEDs as the illumination light source and the InGaAs detector as the detector. For all experiments the measured spectra of the plastic samples are SNV filtered. The data is filtered with the following equation:

$$\text{output data} = \frac{\text{input data} - \text{mean input data}}{\text{standard deviation}} \tag{3.1}$$

in which the output data is the SNV-filtered data, the input data is the measured data set of one plastic sample, the mean input data is the determined mean of the input data set and the standard deviation is the determined standard deviation of the input data set. By SNV filtering the data is compensated for the different reflection intensities [27].

3.3.1   Halogen lamp and NIR spectrometer

The NIR spectra of the types of plastic can be measured with a NIR spectrometer, a broadband light source and an optical reflection probe. The probe is able to illuminate the plastic and detect the reflected NIR spectra. The equipment needed to execute the experiment are as follows:

- Plastic sample reference box C (containing PET, HDPE, PVC, LDPE, PP and PS)

- Avantes NIR spectrometer (AVASPEC-NIR256-2.0TEC)

- Halogen lamp (AVALIGHT-HAL LS-1108038)

- Optical reflection probe (FCR-7IR200-2-ME)

- USB-A to USB-B cable

- Stand to hold the probe

- Reference tiles (Avantes, Plastic Scanner, paper sheet, PTFE, Spectrapod)

- Computer/Laptop containing AvaSoft8 software

Setup

The setup is built according to figure 3.5. The probe is connected to the light source and the NIR spectrometer. The end of the probe is held by a clasp to be able to detect the NIR spectrum of the plastic sample from above.
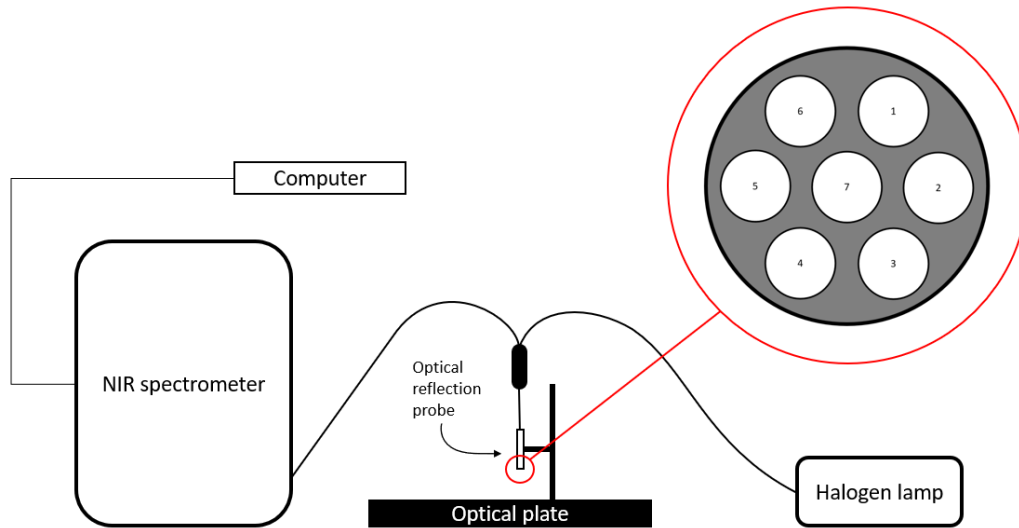
Figure 3.5: A schematic side view of the setup to identify the types of plastic using a NIR spectrometer. An optical reflection probe is connected to the halogen lamp light source and the NIR spectrometer. The ending of the probe is placed in such a way that it can illuminate and detect the plastic samples on the plate. The six fibres inside the probe illuminate the sample and the seventh fibre detects the reflected spectra. A clasp is used to hold the probe ending at a distance of 10 mm from the optical plate. The NIR spectrometer is connected to a computer/laptop containing the AvaSoft8 software.

Before measuring, the integration time and average of the Avantes spectrometer are set. The integration time is set on a value of 80.000 ms and the average is set on a value of 1. The Dynamic Dark in the same settings is disabled. The range of the wavelength in which the spectrometer will measure are set from 1000 nm to 1900 nm. A dark measurement is made and saved in AvaSoft8.

First the reference tiles are measured. The reference tile is placed under the probe ending with a distance in between of 10 mm. The tile is measured five times, where at each measurement a different location on the tile is measured. By measuring the tile five times at different locations, the repeatability of the experiment is taken into account. After measuring each reference tile, the plastic samples provided by Plastic Scanner are measured. Six different plastic types are present in reference box C: PET, HDPE, PVC, LDPE, PP and PS. Each bag consists of four to six samples of one type of plastic. Each sample of the plastic type is measured five times at different locations on the sample. The plastic samples are placed on top of the reference tile that will be used during the experiment. The samples are measured in a continuous scan of the spectrometer.

The data is manually saved in Excel-documents during each measurement and plotted using python.

3.3.2   LEDs and NIR spectrometer

The NIR spectra of the types of plastics are detected using a spectrometer and illuminated with NIR LEDs. An optical multimode fibre is connected between the spectrometer and the LED development board. The equipment needed to measure the spectra of the plastics are as follows:

- Avantes NIR spectrometer (AVASPEC-NIR256-2.0TEC)

- Optical multimode fibre (FC-UVIR400-1-ME)

- NIR LED development board with SMA connection

- Plastic sample reference box C (containing PET, HDPE, PVC, LDPE, PP and PS)

- Reference tile (Avantes, Plastic Scanner, paper sheet, PTFE, Spectrapod)

- USB-A to USB-B cable 2x

- Computer/laptop containing Avasoft8 software and Arduino IDE

- Arduino with software to control the LED development board

- Stand to hold the Arduino

- Stand to hold the LED development board

- Connection cables for the Arduino and development board

Setup

The basis of the setup is derived from figure 3.5. In this setting a single fibre is connected between the LED's development board and the spectrometer in which the spectrometer is used as the detector. A schematic view of the setup is presented in figure 3.6.
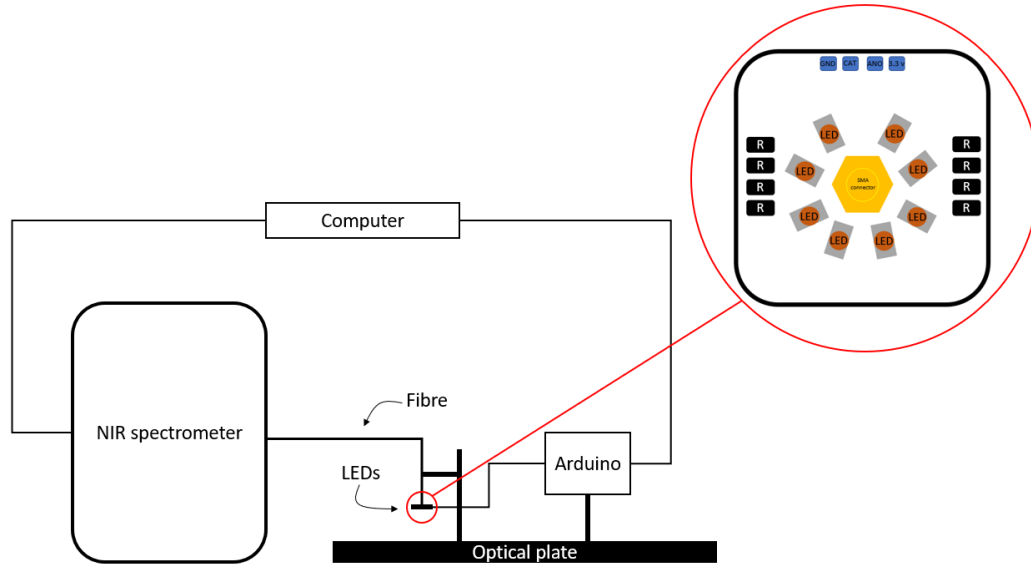
Figure 3.6: A schematic side view of the setup to measure the spectra of the types of plastics using NIR LEDs as the light source. The LEDs are controlled by an Arduino. The Arduino and the spectrometer are connected to a computer containing Avasoft8 and Adruino IDE.

The LED development board and the Arduino development board are mounted to the optical table. The two boards are connected via three electronic cables. Placed on the position A, B and C in figure 3.7. The Arduino is connected to the computer on which the Arduino IDE software is installed. The LED development board is via the SMA connector in 3.7 connected to the NIR spectrometer with an optical fibre. The spectrometer is connected to the computer to measure the reflected spectra from the plastic samples.
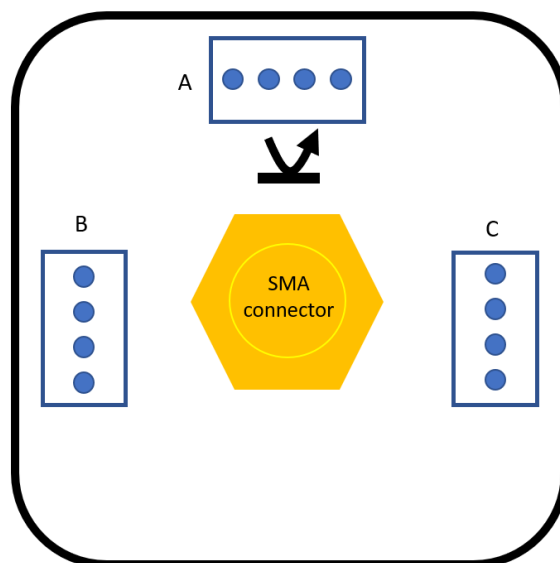
Figure 3.7: The backside of the internal design of the spectroscopic side of the plastic scanner. The blue rectangles (A, B and C) are used to connect the board with the Arduino via the three electronic cables. The optical fibre is connected between the board and the NIR spectrometer using the SMA connector attached to the board.

The LEDs are controlled by the program written in Arduino IDE. First select the board and COM-port belonging to the Arduino connection with the computer. Thereafter, open the "Serial Monitor" in "Tools". The LEDs can be controlled by typing "scan" or "keepscan" as a command in the command bar. By using "scan" as a command each LED is turned on once for 10 ms. By using "keepscan" as a command, the Arduino will run a 10 second long illumination cycle of the LEDs. One LED illumination cycle is 64 ms in which each LED is lit for 8 ms. The illumination cycle is repeated for 10 seconds. The spectra of the plastic samples is measured with the spectrometer in which the integration time is set on 2.560 seconds. During the 10 seconds the spectrum of the plastic sample can be manually saved in an Excel-document in the AvaSoft8 program. The data is then processed in python.

3.3.3   Plastic scanner

The spectra of the types of plastic are measured using the prototype of the plastic scanner. The plastic scanner is controlled by the PS plot program available on GitHub. The equipment needed to measure the spectra of the plastic with the plastic scanner are as follows:

- Plastic scanner prototype #01

- Plastic sample reference box C (containing PET, HDPE, PVC, LDPE, PP and PS)

- Reference tiles (Avantes, Plastic Scanner, paper sheet, PTFE, Spectrapod)

- USB-A to USB-B cable

- Computer/laptop containing PS plot software

Setup

The spectra of the types of plastic is measured by using a prototype of the plastic scanner. Figure 3.8 shows a schematic view of the setup for executing the experiment.
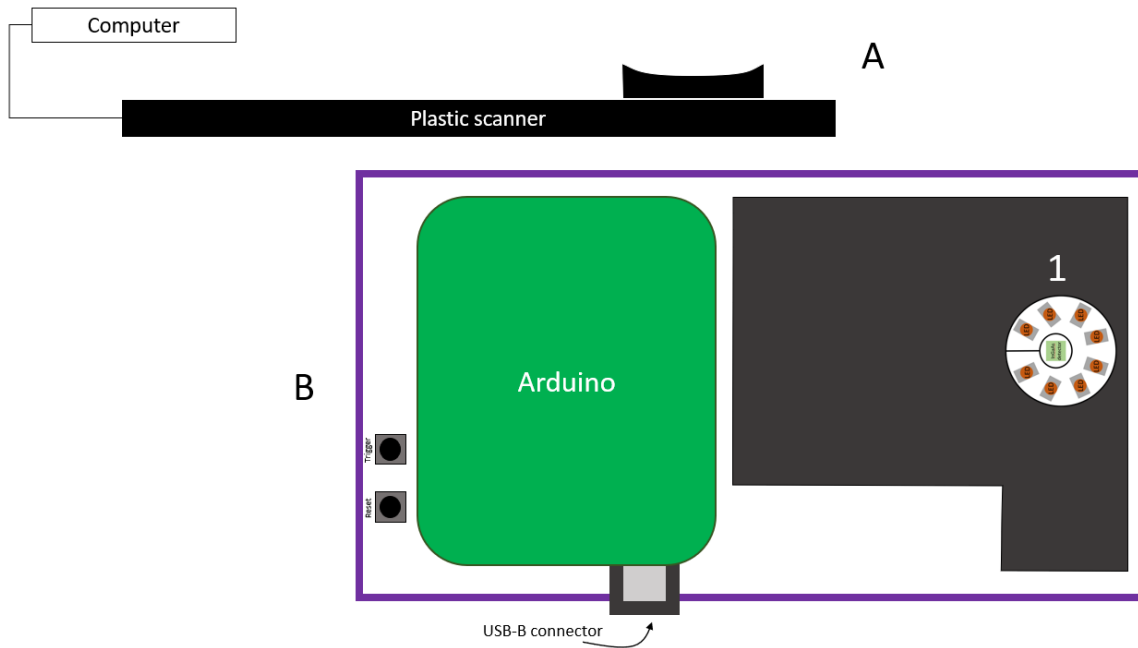

Figure 3.8: A schematic side and top view of the setup to identify the types of plastic using the plastic scanner. **A** is the side view of the plastic scanner. **B** is the top view of the plastic scanner in which **1** is the scanning area. The increment in **A** represents the 10 mm spacer of **1**. The plastic scanner is through the USB-B connector via a USB-A to USB-B connector connected to the computer.

The prototype of the plastic scanner is connected to a computer containing the PS plot software which can be found on GitHub [28]. To use the real data in PS plot, the correct COM-port needs to be selected. This can be done at the top of program format, see figure 3.9.
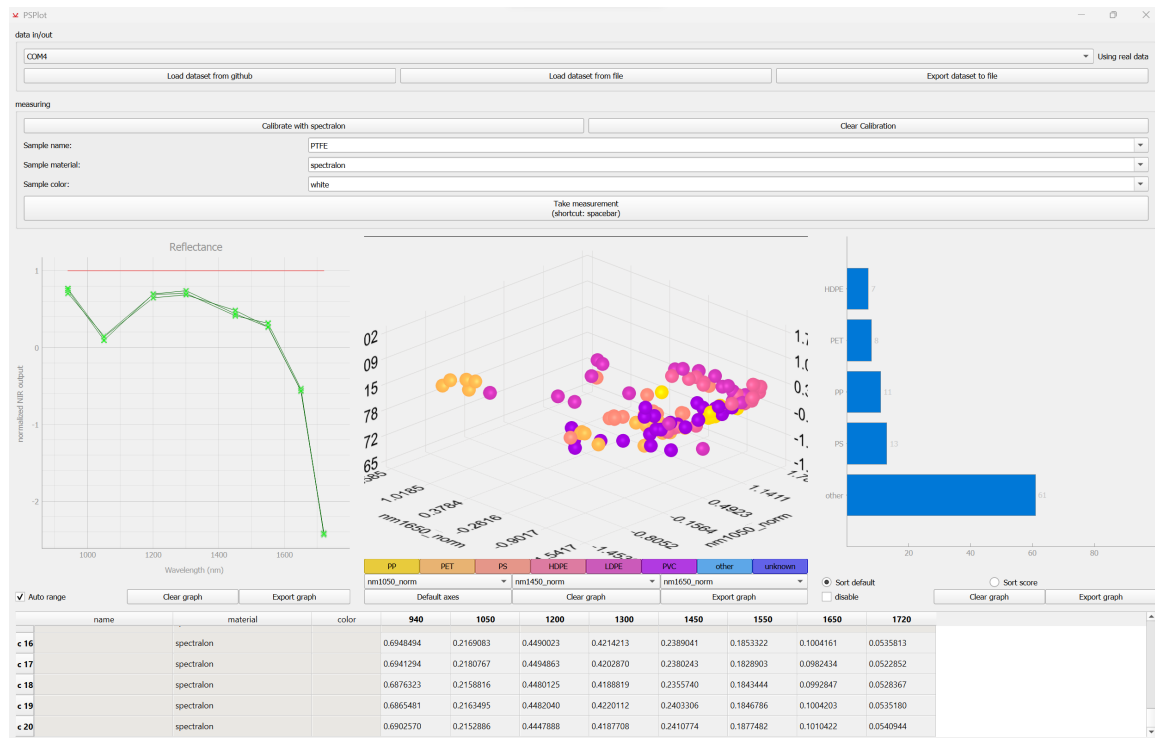
Figure 3.9: A screen shot of the PS plot program. The graph on the left shows the measured spectra of the samples with the red line as the reference. The middle graph shows the measurement points in a 3D plot with the axis indicating the intensity of the dips in the spectra. The right graph is a probability graph, in which the bars indicate by what percentage the sample corresponds to a type of plastic. The data underneath the graphs are the raw output of the InGaAs detector. An enlarged figure can be found in appendix A.

The reference tiles are measured before the plastic samples. Each tile is placed on top of the scanning area (**1** in figure 3.8). By pressing the "Calibrate with spectralon" button, a measurement of the reference tile will be taken. The red line in the left graph will appear. After calibrating, the plastic samples can be measured by laying the samples on the scanning area and putting the reference tile on top of the sample. The identification code and features of the sample can be put in the bars above the measurement button. Each reference tile and plastic sample will be measured five times. After each five measurements the data is manually copied, pasted and saved in a .txt-file. At the end of all measurements the data can be exported to a .csv-file using the "Export dataset to file" button in the right corner. The data from the .txt-files is then processed in python.

4   Results

Within this section the results of the characterisation of the LEDs and InGaAs detector, the results of the reflection spectra of the different types of plastic and the differences in measuring with the plastic scanner versus the NIR spectrometer will be discussed.

4.1   LEDs and InGaAs detector characterisation

To determine if the spectra, Full Width Half Maximum (FWHM) and the peak wavelength of the LEDs correspond with the data sheet, the spectra of the LEDs have been measured using a spectrometer. The results of this experiment are presented in this section.

The spectra of the 940 nm and the 1050 nm LEDs have been measured using a spectrometer with a detection range between 300 nm to 1100 nm. The spectra of the 1200 nm to 1720 nm LEDs have been measured with an NIR spectrometer with a detection range between 1000 nm to 2000 nm. The spectra of all LEDs are plotted in a single graph presented in figure 4.1a. The responsivity of the InGaAs is plotted in 4.1b.
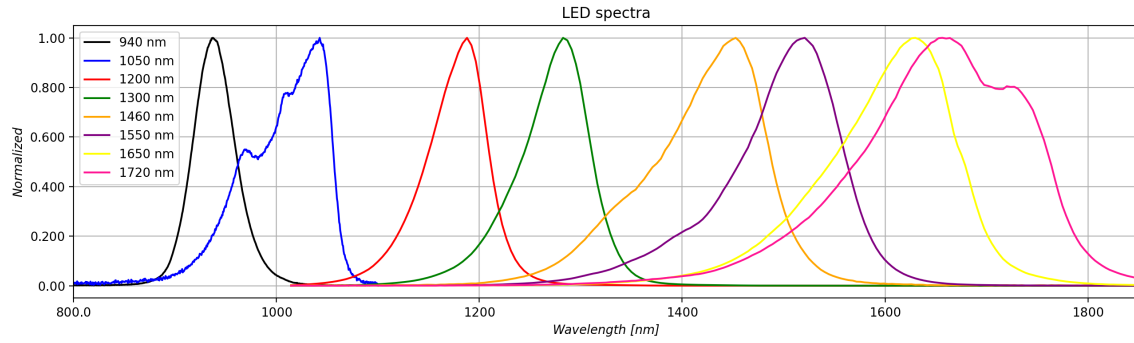
(a) The measured LED spectra plotted in a single graph. The reflectance has been normalised.
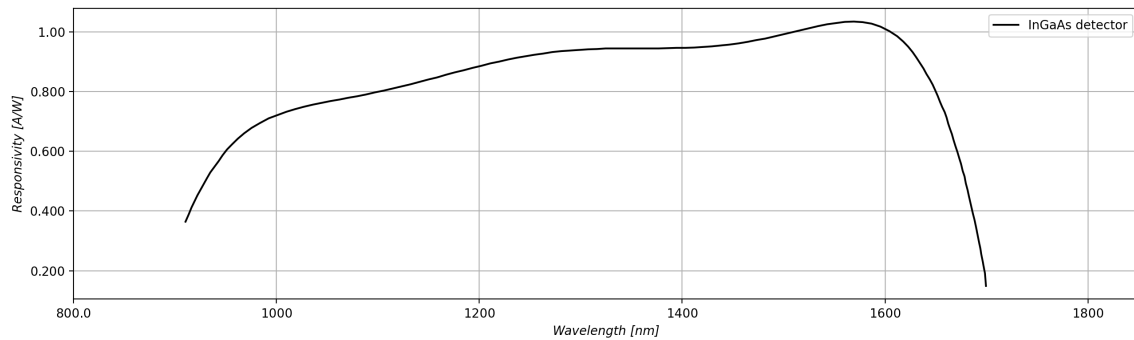
(b) The responsitivity of the InGaAs detector plotted with the extracted data from the data sheet.

Figure 4.1: The spectra of the LEDs and the responsivity of the InGaAs detector plotted with the same x-axis. (a) shows that the spectra overlap over a range of 900 nm to 1800 nm except at around 1100 nm and around 1350 nm. The spectra of the 1650 nm LED and the 1720 nm LED overlap almost entirely. (b) shows the responsivity of the InGaAs detector over a range of 900 nm to around 1700 nm.

The x-axis of both figures are equal to represent how much of the spectra of the LEDs can be detected by the detector. Figure 4.1a shows the normalised spectra of the 8 different LEDs. The figure shows that the spectra overlap at most wavelengths except around 1350 nm and even less at 1100 nm. The spectra of the 1650 nm and 1720 nm LED overlap almost entirely. For this reason, we may consider removing one of the LEDs from the design. Considering the responsivity of the detector, figure 4.1 shows that the spectra of the outer LEDs cannot be fully detected by the detector.

The responsivity of the data sheet starts at 900 nm compared to the 800 nm of the responsivity in the theory.

UITLEGGEN. WAT IS ZICHTBAAR EN WAT BETEKEND DAT.

To determine whether the measured spectra match the spectra from the data sheet, the FWHM values and the peak values of the wavelengths are compared. Figures 4.2 and 4.3 show the comparison between the determined values and the values from the
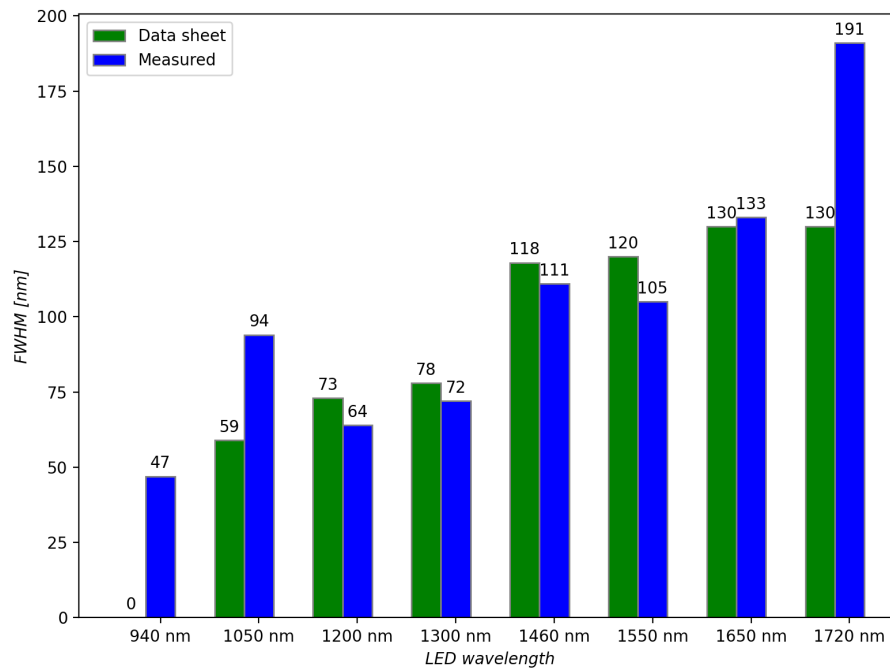
29

data sheet.

Figure 4.2: The FWHM values plotted as a bar graph to visualise the deviation between the determined values and the values obtained from the data sheet.

It was to be expected that the determined FWHM values would correspond with the FWHM values obtained from the data sheet. However, it can be seen in figure 4.2 that the deviations vary between 3 nm to 61 nm. The 1720 nm LED has the largest deviation from the data sheet.

The peak wavelengths of both the determined values as the obtained values from the data sheet are presented in figure 4.3.
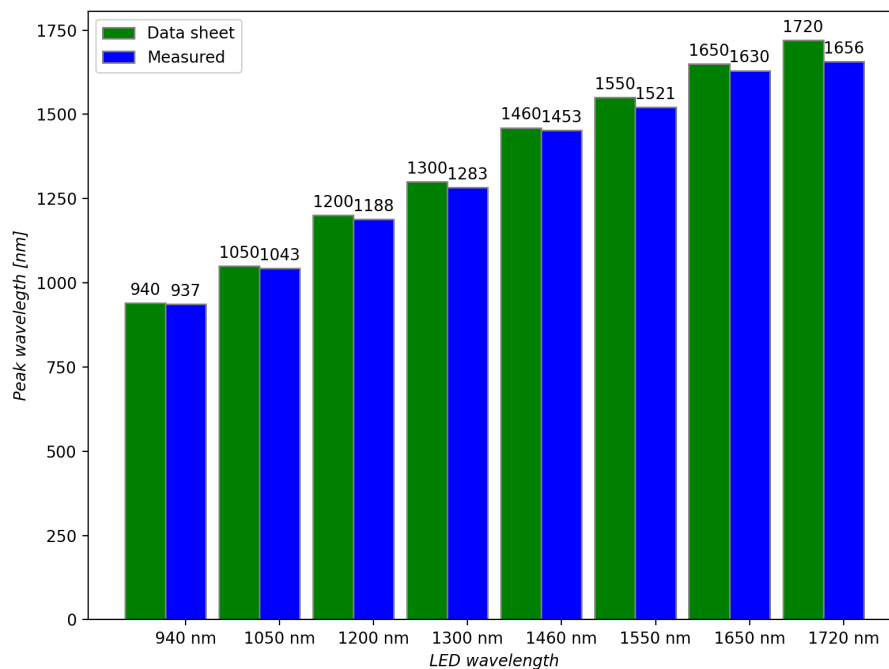
Figure 4.3: The peak wavelengths plotted as a bar graph to visualise the deviation between the measured data and the data obtained from the data sheet.

The deviations between the obtained and determined values vary between 3 nm to 64 nm. This is not as expected. The 1720 nm LED has the largest deviation of 64 nm. The 940 nm LED has the smallest deviation of 3 nm. For all LEDs the measured peak wavelength is lower than the peak wavelengths obtained from the data sheet.

NIETZEKER OF FIGUREN OF TABELLEN OVERZICHTELIJKER ZIJN VOOR DE INFO VAN FWHM EN PEAK WAVELENGTH. WAT BETEKEND DE INFORMATIE IN DIE FIGUREN/TABELLEN

4.2 Plastic identification

VERSCHILLEN BENOEMEN TUSSEN DE PLASTIC SCANNER EN DE AVANTES METING. To determine the spectra of the plastic samples, the samples have been measured with a halogen light and LEDs as a light source, where the NIR spectrometer was used as the detector. The samples have also been measured using a prototype of the plastic scanner, where the LEDs are used as a light source with the InGaAs detector as the detector. The spectra of the types of plastic of the three different experiments are shown in figure 4.4.

(a) Measured with a halogen lamp as a light source and the NIR spectrometer as the detector.

(b) Measured with the LEDs as a light source and the NIR spectrometer as the detector.

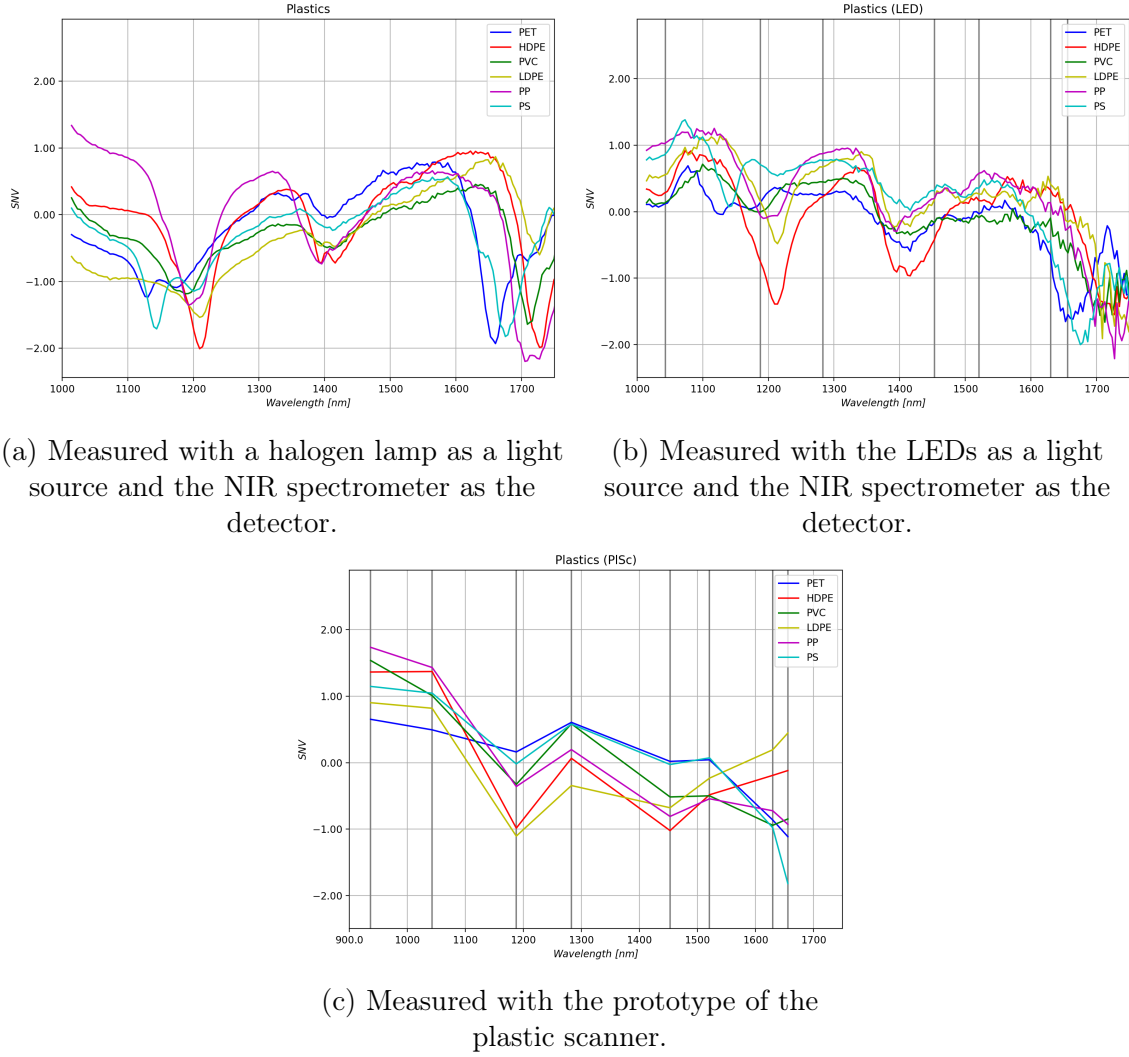(c) Measured with the prototype of the plastic scanner.

Figure 4.4: The spectra of the different types of plastic plotted against the wavelength. The spectra of the plastics have been measured using a halogen lamp as a light source and the NIR spectrometer as the detector. A SNV-filter was applied to the plotted data sets.

In figure 4.4a a halogen lamp and a NIR spectrometer were used to measure the reflection spectra of the different types of plastic. The figure shows that identification dips of the types of plastic are between 1100 nm to 1250 nm, around 1400 nm and between 1600 nm to 1750 nm. The reflection spectra of the types plastic in figure 4.4b have been measured using a LED development board and a NIR spectrometer. This figure also shows the identification dips around 1400 nm and between 1600 nm to 1750 nm. The dips between 1100 nm to 1250 nm that are visible in figure 4.4a are in figure 4.4b more centred around the 1200 nm. Figure 4.4b also shows that there is noise present in the reflected spectra. A cause could be the low power emitted by the 1650 nm and 1720 nm LEDs. The noise is also present around 1100 nm, where the spectra of the LEDs do not overlap. Figure 4.4c shows the reflection spectra measured with

a prototype of the plastic scanner. The plastics can be best distinguished looking at the spectra at 937 nm and 1656 nm. At these wavelengths the spectra do not overlap with each other.

DE 10 MM BLIJFT MEER CONSICENT BEHOUDEN BIJ DE PLASTIC SCAN-NER DAN BIJ DE EXPERIMENTEN WAAR ER GEBRUIK IS GEMAAKT VAN DE SPECTROMETER

Figures 4.4a and 4.4b show for all spectra a dip around the 1400 nm. This suggests that it would be more beneficial to replace the 1450 nm LED with a 1400 nm LED to gain more intensity around the dip. To determine if the measured spectra belong to the type of plastic, the spectra are compared to the theory. The theoretic spectra are shown in figure 4.5.
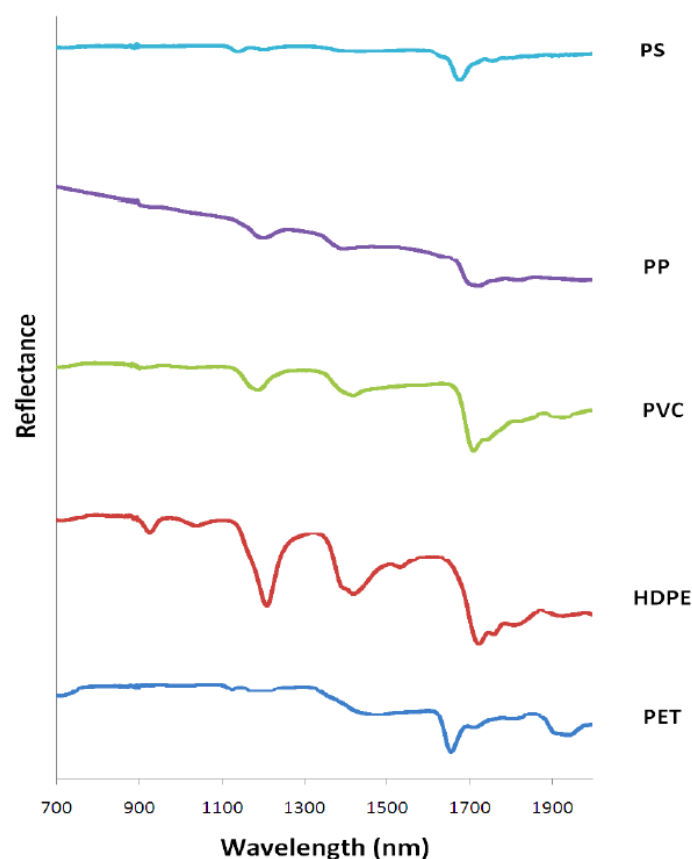

Figure 4.5: The reflectance of five of the most common types of plastic. The spectra are plotted with an offset to avoid interference and enhance clarity. [20]

Figure 4.5 shows that the 940 nm LED in the plastic scanner is needed to distinguish the spectrum of the HDPE from the spectrum of the PVC. However, the dip is not visible in the results measured with the spectrometer because of the detection limit of the NIR spectrometer.

The reference tile of the Plastic Scanner was used as the reference tile for under the plastic samples or atop of the plastic samples.

4.2.1   Plastic characteristics

From each type of plastic not every samples should be used for the reference box. The following samples show a spectrum that do not show all of the identification dips to distinguish the types of plastic:

Table 4.1: Caption

Sample code	Colour
A05C	green
B05C	grey
C05C	blue
C06C	grey
D01C	white
D02C	transparent
F02C	blue

The spectra of these samples can be found in appendix B. For most samples the darker coloured samples have a less defined spectrum, except for the two samples of LDPE. A reason for these undefined spectra could be of the thickness of the sample.

IETS ZEGGEN OVER DE AFSTAND TUSSEN DE SAMPLE EN DE SCANNER (INTENSITEIT VAN DE REFELCTIE VERSCHILT, SPECTRA BLIJFT HELTZELFDE)

VERSCHILLENDE REFERENTIE TEGELS BENOEMEN DIE GEBRUIKT ZIJN EN WAAROM DE KEUZE IS GEMAAKT VOOR PS TEGEL

WELK EFFECT HEEFT DE KLEUR VAN HET PLASTIC OP HET METEN VAN DE SPECTRA. FIGUREN LATEN ZIEN WAARBIJ DONKERE KLEUREN GEEN SPECTRUM LEVEREN.

4.3   Discussion

5   Conclusion

Most LEDs are correctly chosen. Whether the 1650 nm LED is useful for identification of plastic types can be questioned. Since the 1650 nm and 1720 nm LED almost completely overlap, either one can be used for identification. Of both LEDs, part of the spectrum falls outside the range of the detector.

The results also show that an identification dip is visible at 1400 nm. It would be wise to switch the LED from 1460 nm to 1400 nm to get more intensity around 1400 nm. The noise in the spectra at the last two LEDs is caused by the low intensity of the LEDs. By increasing the intensity, clearer spectra can be measured. It is therefore recommended to replace the LEDs of 1650 nm and 1720 nm with an LED of higher power.

The distance between the plastic sample and the scanner is better achievable with the plastic scanner than with reference setup. This because not every piece of plastic is flat and still could cause a distance decrease. With the plastic scanner, the sample can be touched and a smaller area is scanned.

5.1   Recommendations

Use 1400 nm LED. Find higher power LEDs for 1650 nm and 1720 nm. Which samples should be in the reference box. Table 4.1

References

[1] L. Parker, "The world's plastic pollution crisis explained," *Environment*, May 2021. [Online]. Available: https://www.nationalgeographic.com/environment/article/plastic-pollution

[2] "Plastic Scanner. | Plastic Scanner," Apr. 2023, [Online; accessed 26. Apr. 2023]. [Online]. Available: https://plasticscanner.com

[3] "Plastic Waste and Pollution [Everything You Need To Know In 2020]," Nov. 2022, [Online; accessed 16. May 2023]. [Online]. Available: https://cleanstreets.westminster.gov.uk/plastic-waste-complete-guide/#2

[4] admin, "Plastics – Resin Codes. What do they mean? - 2EA," *2EA*, Jan. 2018. [Online]. Available: https://2ea.co.uk/plastics-resin-codes-what-do-they-mean

[5] "Plastic Recycling Codes & Symbols Explained - Plastic Soup Foundation," May 2020, [Online; accessed 16. May 2023]. [Online]. Available: https://www.plasticsoupfoundation.org/en/plastic-problem/what-is-plastic/recycling-codes

[6] A. Straller and B. Gessler, "Identification of Plastic Types Using Discrete Near Infrared Reflectance Spectroscopy," *ResearchGate*, Dec. 2019. [Online]. Available: https://www.researchgate.net/publication/337868860_Identification_of_Plastic_Types_Using_Discrete_Near_Infrared_Reflectance_Spectroscopy

[7] "About | Plastic Scanner," Jan. 2023, [Online; accessed 9. Feb. 2023]. [Online]. Available: https://plasticscanner.com/about

[8] N. Gorretta, A. A. Gowen, N. Holden, M. Wolfe, J. Ogejo, and E. E. Cummins, "Visible and near infrared optical spectroscopy sensors for biosystems engineering," 2020.

[9] "Overview | Plastic Scanner documentation," May 2023, [Online; accessed 16. May 2023]. [Online]. Available: https://docs.plasticscanner.com

[10] "Science of Plastics," Nov. 2019, [Online; accessed 9. Feb. 2023]. [Online]. Available: https://www.sciencehistory.org/science-of-plastics

[11] "An Introduction to Plastics - Chemical Safety Facts," Oct. 2022, [Online; accessed 9. May 2023]. [Online]. Available: https://www.chemicalsafetyfacts.org/chemistry-101/an-introduction-to-plastics

[12] NPO Kennis, "Wat is plastic en hoe maak je het?" *NPO Kennis*, Jan. 2022. [Online]. Available: https://npokennis.nl/longread/7956/wat-is-plastic-en-hoe-maak-je-het

[13] "Polyethylene Terephthalate - an overview | ScienceDirect Topics," Feb. 2023, [Online; accessed 9. Feb. 2023].

[14] "Polyvinyl Chloride Structure & Uses | What is PVC? | Study.com," Feb. 2023, [Online; accessed 9. Feb. 2023]. [Online]. Available: https://study.com/learn/lesson/what-is-polyvinyl-chloride-pvc-structure-uses.html

[15] "Polypropylene (PP) - Types, Properties, Uses & Structure," Feb. 2023, [Online; accessed 9. Feb. 2023]. [Online]. Available: https://omnexus.specialchem.com/selection-guide/polypropylene-pp-plastic

[16] "A Polystyrene Model of Polystyrene Tacticity," Nov. 2021, [Online; accessed 9. Feb. 2023]. [Online]. Available: https://www.chemedx.org/blog/polystyrene-model-polystyrene-tacticity

[17] "Polyethylene (PE) - Properties, Uses & Application," Feb. 2023, [Online; accessed 9. Feb. 2023]. [Online]. Available: https://omnexus.specialchem.com/selection-guide/polyethylene-plastic

[18] D. ir. M.T.C. de Loos-Vollebregt, *Spectrometrische analysetechnieken*. Arnhem: Syntax Media, 2009.

[19] O. c. Tutor, "Infrared Spectroscopy - Online Organic Chemistry Tutor," *Online Organic Chemistry Tutor*, Nov. 2017. [Online]. Available: https://onlineorganicchemistrytutor.com/infrared-spectroscopy

[20] H. Masoumi, S. M. Safavi, and Z. Khani, "Identification and classification of plastic resins using near infrared reflectance spectroscopy," *International Journal og Mechanical and Industrial Engineering*, vol. 6, pp. 213–220, 2012.

[21] "Infrared Spectroscopy," Dec. 2010, [Online; accessed 23. May 2023]. [Online]. Available: https://www.ru.nl/systemschemistry/equipment/optical-spectroscopy/infrared

[22] "What is Spectroscopy? - Avantes," Sep. 2022, [Online; accessed 23. May 2023]. [Online]. Available: https://www.avantes.com/what-is-spectroscopy

[23] S. Kasap, *Optoelectronics and Photonics: Principles and Practices*, 2nd ed. Pearson Education Limited, 2013, ch. 3.

[24] D. C. Giancolli, *Physics for Scientists & Engineers with Modern Physics*, 4th ed. Pearson Education Inc., 2009, ch. 40.

[25] S. Kasap, *Optoelectronics and Photonics: Principles and Practices*, 2nd ed. Pearson Education Limited, 2013, ch. 5.

[26] A. Rohatgi, "WebPlotDigitizer - Copyright 2010-2022 Ankit Rohatgi," Sep. 2022, [Online; accessed 21. Apr. 2023]. [Online]. Available: https://apps.automeris.io/wpd

[27] Bijdragers aan Wikimedia projecten, "Standard Normal Variate - Wikipedia," Apr. 2017, [Online; accessed 15. May 2023]. [Online]. Available: https://nl.wikipedia.org/w/index.php?title=Standard_Normal_Variate&oldid=48942585

[28] "Plastic-Scanner · GitHub," May 2023, [Online; accessed 11. May 2023].
[Online]. Available: https://github.com/Plastic-Scanner
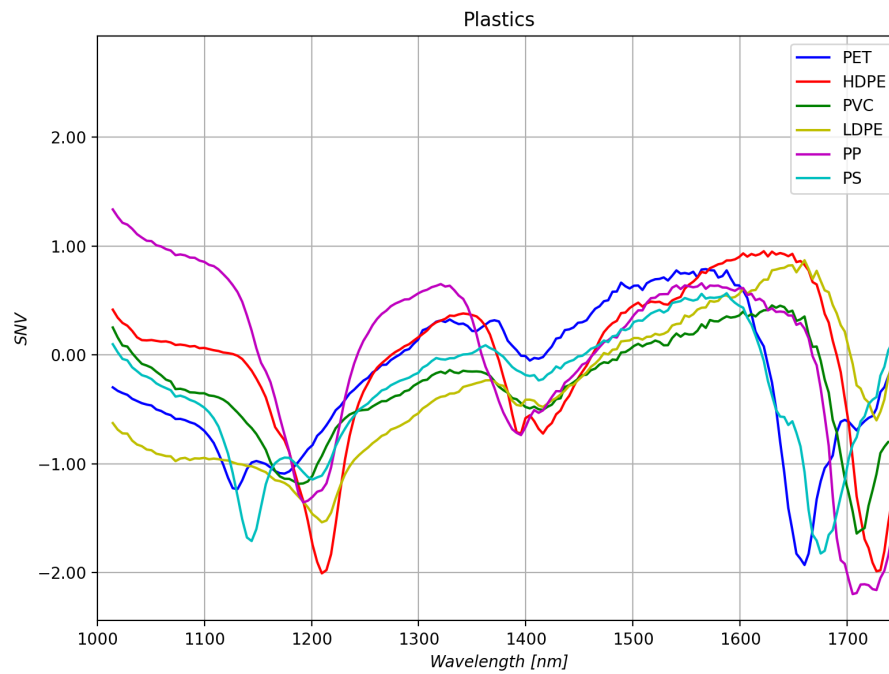
Appendices
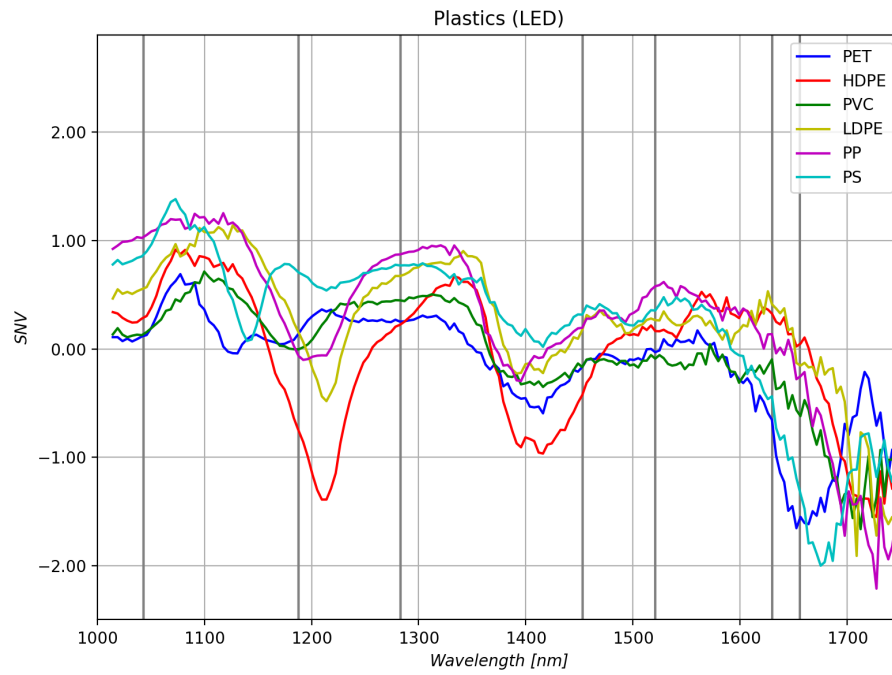
A   Enlarged figures
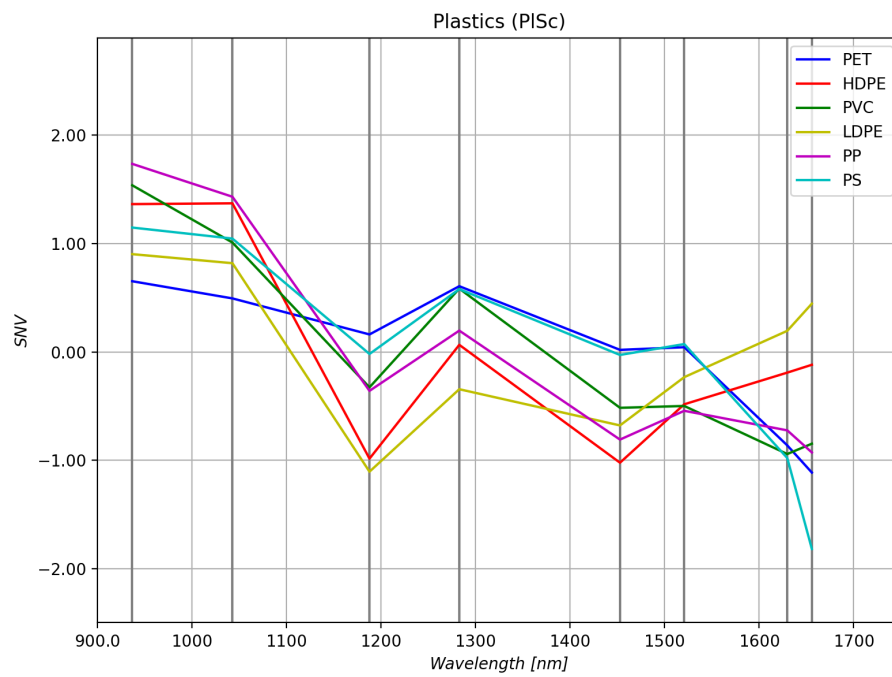

Figure A.1: Caption

Figure A.2: Caption

Figure A.3: Caption

Figure A.4: Caption

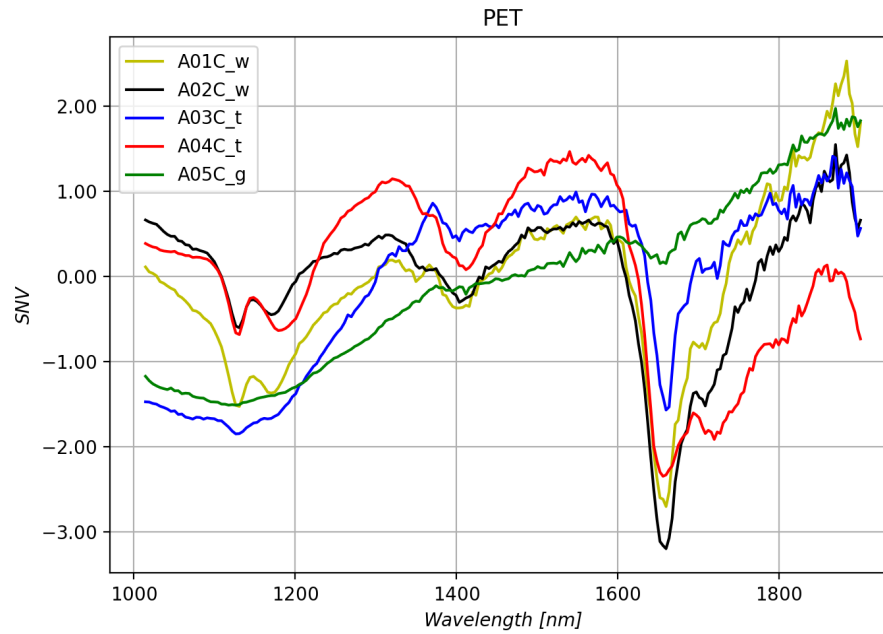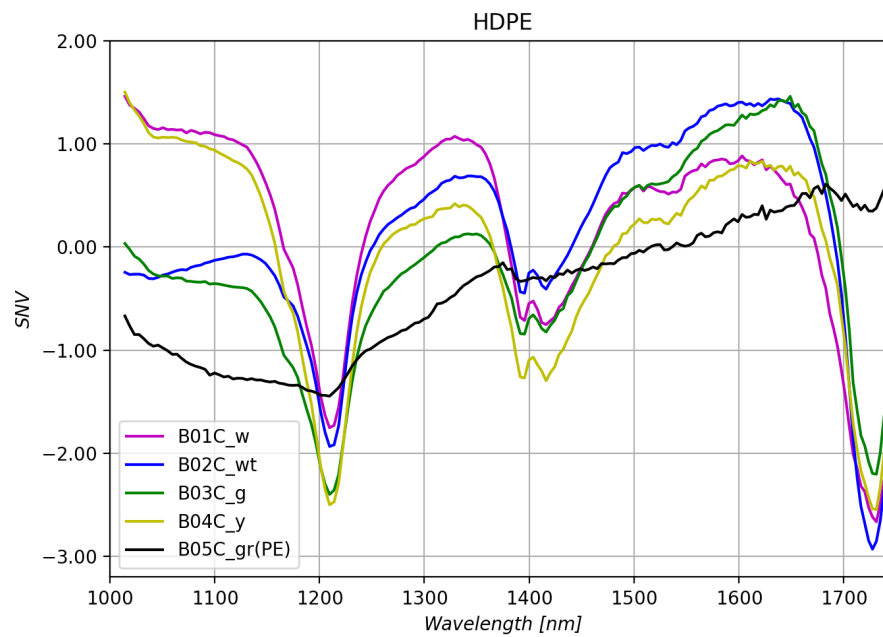# B   Figures of the plastic characteristics
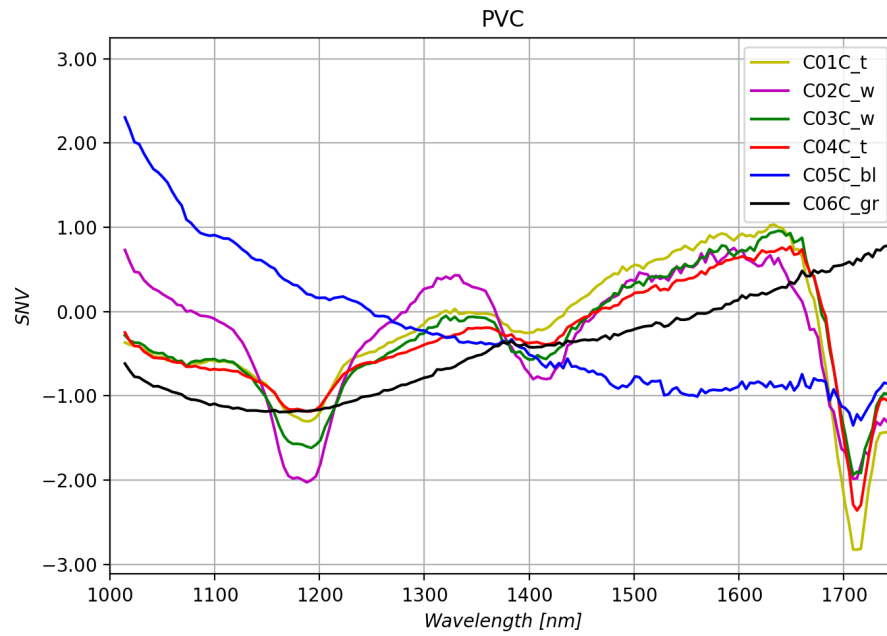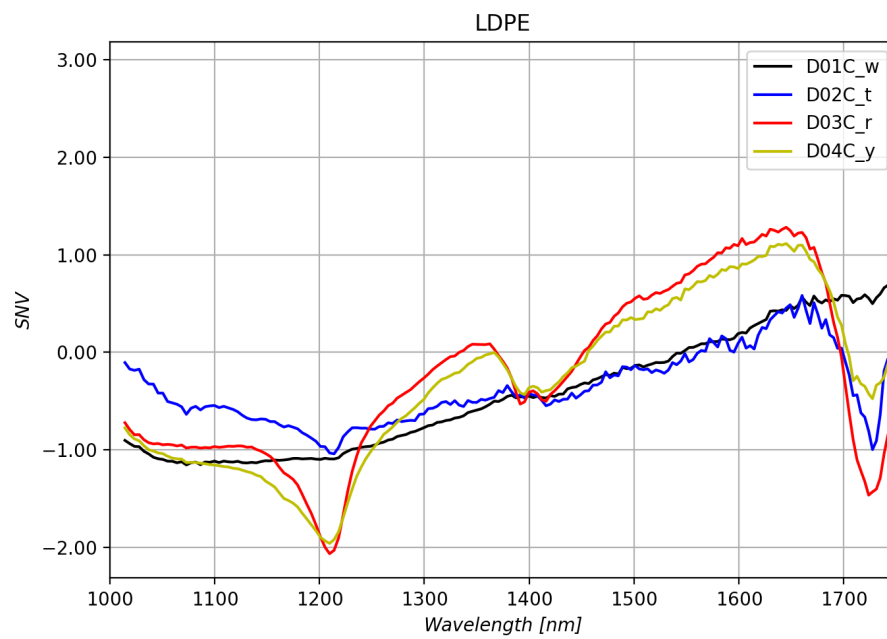

Figure B.1: Caption
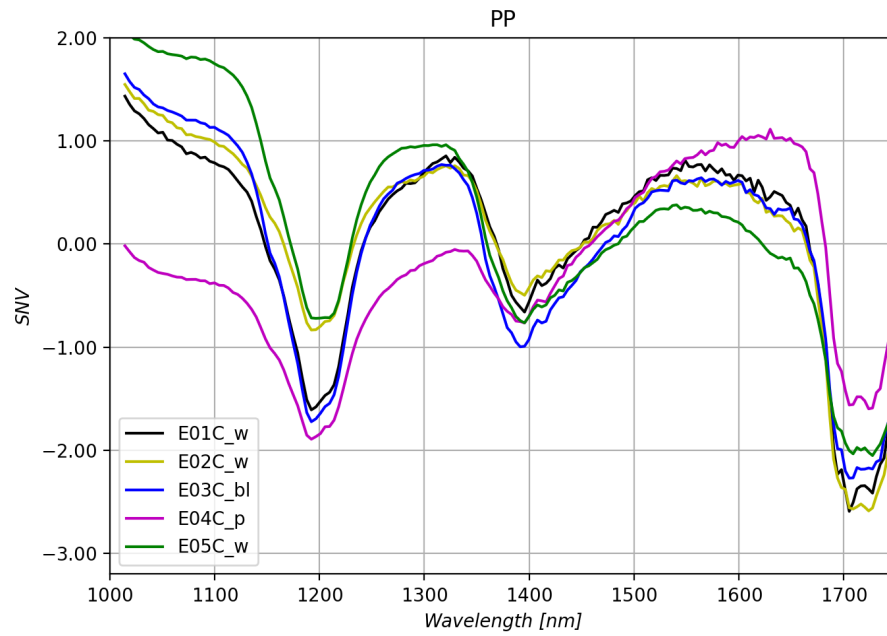

Figure B.2: Caption

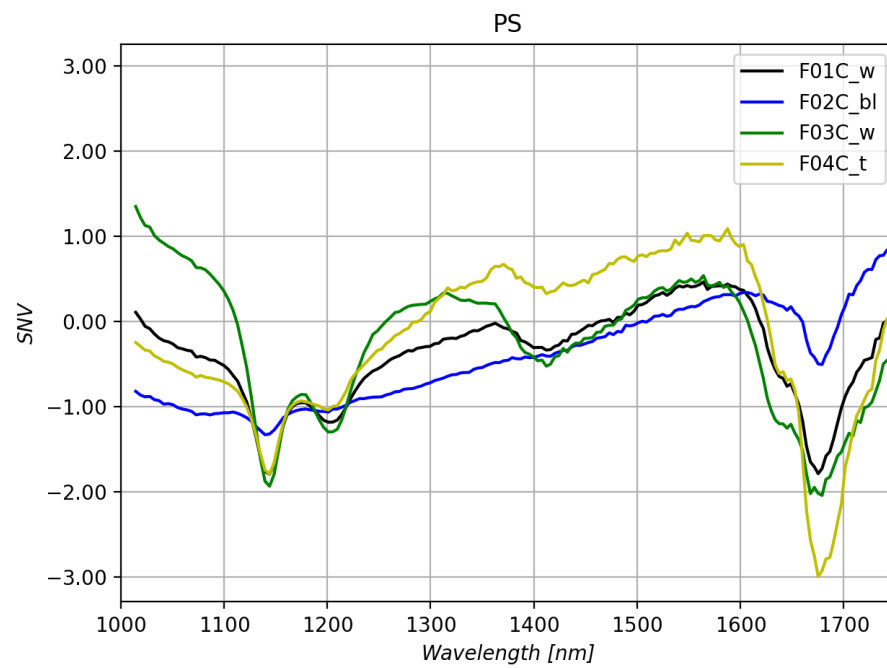Figure B.3: Caption

Figure B.4: Caption

Figure B.5: Caption

Figure B.6: Caption